

SYNTHESIS OF LITHIUM BORIDES BY MECHANOCHEMICAL PROCESS

A THESIS SUBMITTED TO
THE GRADUATE SCHOOL OF NATURAL AND APPLIED SCIENCES
OF
MIDDLE EAST TECHNICAL UNIVERSITY

BY

ONUR ÖNDER

IN PARTIAL FULFILLMENT OF THE REQUIREMENTS
FOR
THE DEGREE OF MASTER OF SCIENCE
IN
METALLURGICAL AND MATERIALS ENGINEERING

FEBRUARY 2009

Approval of the thesis:

**SYNTHESIS OF LITHIUM BORIDES BY MECHANOCHEMICAL
PROCESS**

submitted by **Onur Önder** in partial fulfilment of the requirements for the
degree of **Master of Science in Metallurgical and Materials
Engineering Department, Middle East Technical University** by,

Prof. Dr. Canan Özgen _____
Dean, Graduate School of **Natural and Applied Sciences**

Prof. Dr. Tayfur Öztürk _____
Head of Department, **Metallurgical and Materials Engineering**

Prof. Dr. Ahmet Geveci _____
Supervisor, **Metallurgical and Materials Engineering Dept., METU**

Prof. Dr. Yavuz Topkaya _____
Co-Supervisor, **Metallurgical and Materials Engineering Dept., METU**

Examining Committee Members:

Prof. Dr. Naci Sevinç _____
Metallurgical and Materials Engineering Dept., METU

Prof. Dr. Ahmet Geveci _____
Metallurgical and Materials Engineering Dept., METU

Prof. Dr. Yavuz Topkaya _____
Metallurgical and Materials Engineering Dept., METU

Prof. Dr. İshak Karakaya _____
Metallurgical and Materials Engineering Dept., METU

Prof. Dr. Gülhan Özbayoğlu _____
Mining Engineering Dept., METU

Date: 10.02.2009

I hereby declare that all information in this document has been obtained and presented in accordance with academic rules and ethical conduct. I also declare that, as required by these rules and conduct, I have fully cited and referenced all material and results that are not original to this work.

Name, Last Name : Onur Önder

Signature :

ABSTRACT

SYNTHESIS OF LITHIUM BORIDES BY MECHANOCHEMICAL PROCESS

Önder, Onur

M.Sc., Department of Metallurgical and Materials Engineering

Supervisor: Prof. Dr. Ahmet Geveci

Co-Supervisor: Prof. Dr. Yavuz Topkaya

February 2009, 72 Pages

The aim of this study was to investigate synthesis of lithium borides by mechanochemical synthesis from oxides. Lithium borides have promising properties in the area of high energy additives and hydrogen storage. Lithium oxide (Li_2O), boron oxide (B_2O_3) and Mg were used to synthesize lithium borides. Experiments were conducted in a planetary ball mill under argon atmosphere. Analyses of the products were done by X-ray diffraction and scanning electron microscopy. Trilithium tetradecaboride (Li_3B_{14}) peaks were observed in the product powder. Removal of other phases that were formed during experiments was done by leaching in HCl/water solution. Leaching in 0.5 M HCl/water solution for 10 minutes was found to be sufficient to remove; iron (Fe) and magnesium oxide (MgO). Effects of ball

milling parameters such as milling speed, ball to powder ratio, milling duration were investigated and milling for 20 hours with 300 rpm and 30:1 ball to powder ratio was found to be the optimum conditions. Syntheses of other lithium borides (LiB_4 , Li_2B_6 , LiB_{13}) were also experimented with the same milling parameters. Formation of LiB_4 , Li_2B_6 and LiB_{13} was not observed in the product powders. However, the results of LiB_4 and LiB_{13} production experiments showed also Li_3B_{14} peaks in the product. Li_2B_6 synthesis experiments resulted in Li_2B_9 peaks in the product powders.

Keywords: Lithium borides, trilithium tetradecaboride, mechanochemical synthesis, acid leaching.

ÖZ

MEKANOKİMYASAL YÖNTEM İLE LİTYUM BORÜRLERİN SENTEZİ

Önder, Onur

Y. Lisans, Metalurji ve Malzeme Mühendisliği Bölümü

Tez Yöneticisi : Prof. Dr. Ahmet Geveci

Ortak Tez Yöneticisi : Prof. Dr. Yavuz Topkaya

Şubat 2009, 72 Sayfa

Bu çalışmanın amacı mekanokimyasal yöntem ile lityum borür sentezinin araştırılmasıdır. Lityum borürler hidrojen depolama ve yüksek enerjili katkı maddesi gibi konularda gelecek vaadeden özellikler göstermektedir. Deneylerde lityum borür sentezi için girdi malzemeleri olarak lityum oksit (Li_2O), bor oksit (B_2O_3) ve magnezyum kullanılmıştır. Mekanokimyasal yöntem deneyleri bilyalı öğütücü kullanılarak argon gazı altında gerçekleştirilmiştir. Deney ürünleri X-ışını kırınım yöntemi ve taramalı elektron mikroskopisi ile analiz edilmiştir. X-ışını kırınımı analizi sonucunda ürün diyagramlarında trilyum tetradekaborür (Li_3B_{14}) pikleri gözlenmiştir. Deneyler sonunda oluşan diğer fazlar HCl/su çözeltisinde liç edilerek giderilmiştir. Oluşan, demir (Fe) ve magnezyum oksitin giderilmesi için ürünlerin 0.5M HCl/su çözeltisi içinde 10 dakika süre ile liç edilmesinin yeterli olduğu gözlenmiştir. Öğütme parametrelerinin lityum borür

sentezine etkisi de bu alıřmada incelenmiřtir. tme hızı, bilya-toz oranı, tme sresinin etkileri incelenmiř; 300 devir/dakika hızında ve 30:1 bilya-toz oranıyla, 20 saat sre ile tme optimum kořullar olarak belirlenmiřtir. Dięer lityum borrlerin (LiB_4 , Li_2B_6 , LiB_{13}) sentezi aynı tme deęerleri kullanılarak denenmiř, fakat bu bileřiklerin oluřumu gzlenememiřtir. LiB_4 ve LiB_{13} deney rnlerinin X-ıřını kırınımı diyagramlarında Li_3B_{14} pikleri olduęu grlmřtr. Li_2B_6 oluřumu iin yapılan deneyler sonucunda ise rn diyagramlarında Li_2B_9 pikleri gzlemlenmiřtir.

Anahtar Kelimeler: Lityum borrler, trilitiyum tetradekaborr, mekanokimyasal sentez, asit lii.

**To my family
&
My love Görkem P. Yılmaz**

ACKNOWLEDGMENTS

I would like to express the deepest appreciation to Prof. Dr. Ahmet Geveci who has always assisted and guided me in my research. I would also like to thank Prof. Dr. Yavuz Topkaya for his guidance and solving problems that I have faced during my study.

In addition, I am very grateful to Barış Akgün and Çağla Özgüt for their motivation, patient support and valuable discussions. I also should thank to Necmi Avcı for XRD analyses, Cengiz Tan and Metehan Erdoğan for SEM-EDS analyses.

I must thank to Deniz Keçik, Gülhan Çakmak and Hasan Akyıldız for their valuable discussions and support.

I would like to express my deepest gratitude to Görkem Pınar Yılmaz for her love, encouragement and cheering me up in every single moment of my life.

I would like to thank to my best friends Fırat Kadioğlu, Cemal Ökmen Yücel, Bora Mutluer, Tolga Kobaş and Doğan Güngör for sharing the life.

And finally, I offer sincere thanks to my father, my mother and my big brother for their endless patience and encouragement. I especially thank to my uncle Murat Önder for his great help during my study.

TABLE OF CONTENTS

ABSTRACT	iv
ÖZ	vi
ACKNOWLEDGMENTS	ix
TABLE OF CONTENTS	x
LIST OF TABLES	xii
LIST OF FIGURES	xiii
CHAPTER	
1.INTRODUCTION.....	1
2.LITERATURE REVIEW.....	4
2.1 Introduction.....	4
2.2 Classification of borides	4
2.3 Preparation of borides	7
2.4 Lithium borides	10
2.5 Mechanochemical synthesis	19
3.EXPERIMENTAL.....	22
3.1 Input materials	22
3.1.1 Calcination of boric acid	22
3.1.2 Preparation of reactant mixture.....	24
3.2 Ball milling	25
3.3 Ball Milling for Mechanochemical Process	28

3.4 Leaching process.....	30
3.5 Analysis Methods	33
4.RESULTS AND DISCUSSION.....	35
4.1 Introduction.....	35
4.2 Effect of ball mill speed	35
4.3 Effect of leaching parameters.....	41
4.4 Effect of ball to powder weight ratio.....	45
4.5 Effect of excess magnesium.....	48
4.6 Variations in reactant mixture	51
4.7 Other observations.....	63
5.CONCLUSIONS.....	65
REFERENCES.....	67

LIST OF TABLES

Table 2.1. Classification of borides according to Kiessling ⁽¹²⁾	6
Table 2.2. Periodic classification of borides ⁽¹²⁾⁽¹⁴⁾	7
Table 3.1. Properties of powders.....	25
Table 3.2. Chemical analysis of grinding jar and balls ⁽⁶⁵⁾	25
Table 3.3. Ball mill parameters.....	29
Table 3.4. Experimental parameters used.....	29
Table 4.1. Comparison of reaction mixtures (4.3) and (4.1).....	50
Table 4.2. Comparison of reaction mixtures (4.5) and (4.1).....	59

LIST OF FIGURES

Figure 2.1. a) α -Rh Boron ⁽⁴⁴⁾ b) FCC C ₆₀ ⁽⁴⁵⁾	13
Figure 2.2. Structural similarity of β -rhombohedral boron and carbon ⁽⁴⁷⁾	14
Figure 2.3. Formation of B ₈₄ . Two B ₆ units connected to B ₁₂ icosahedra ⁽⁴⁷⁾	14
Figure 2.4. The structures of Li ₃ B ₁₄ boron cluster shown by black lines and the structure of Li _{1.8} B ₁₄ cluster shown by white open lines.....	16
Figure 2.5. Phase diagram of B-Li system ⁽⁵⁴⁾	17
Figure 2.6. Ball to powder collision ⁽⁵⁹⁾	20
Figure 3.1. Pot furnace ⁽¹⁴⁾	23
Figure 3.2. Milling equipment.....	26
Figure 3.3. Retsch PM 100 planetary ball mill ⁽⁶⁶⁾	26
Figure 3.4. Motions of balls in planetary ball mill jar ⁽⁵⁹⁾	27
Figure 3.5. Jar in the ball mill.....	28
Figure 3.6. Leaching equipment.....	32
Figure 3.7. Filtration equipment.....	33
Figure 3.8. Rigaku Multiflex Powder X-ray diffractometer ⁽¹⁴⁾	34
Figure 3.9. Jeol JSM 6400 scanning electron microscope ⁽¹⁴⁾	34
Figure 4.1. X-Ray Diagram for samples ball milled for 20 hours with 30:1 BPR a) 200 rpm, b) 250 rpm, c) 300 rpm, d) 400 rpm.	37

Figure 4.2. X-ray diagram of B_2O_3 after calcination of H_3BO_3	38
Figure 4.3. X-Ray Diagram for samples ball milled for 20 hours with 30:1 BPR a) 300 rpm, b) 400 rpm. Both samples were leached with 0.5 M HCl solution for 10 minutes.....	38
Figure 4.4. X-Ray Diagram for samples ball milled for 20 hours with 30:1 BPR a) 300 rpm, b) 400 rpm. Both samples were leached with 0.5 M HCl solution for 10 minutes.....	39
Figure 4.5. SEM Micrographs for samples ball milled for 20 hours with 30:1 BPR and leached in 0.5 M HCl solution for 10 minutes, a) 300 rpm, b) 400 rpm.....	40
Figure 4.6. X-Ray Diagram for a sample ball milled for 20 hours with 30:1 BPR and 300 rpm	42
Figure 4.7. X-ray diagram for samples that were ball milled for 20 hours with 300 rpm and 30:1 BPR. Products of ball mill were leached with a) 0.375 M, b) 0.5 M, c) 1 M, HCl solutions for 10 minutes	43
Figure 4.8. X-ray diagram for samples that were ball milled for 20 hours with 300 rpm and 30:1 BPR. Products of ball mill were leached with 0.5 HCl/water solutions for a) 10 minutes, b) 30 minutes and c) 60 minutes	45
Figure 4.9. X-ray diagram for samples that were ball milled for 20 hours at 300 rpm with a) 30:1 and b) 60:1 BPR	46
Figure 4.10. X-ray diagram for sample ball milled for 20 hours at 300 rpm. BPR ratios were a) 30:1, b) 45:1, c) 60:1. Products were leached in 0.5 M HCl solution for 10 minutes.....	47
Figure 4.11. X-ray diagram for sample ball milled for 20 hours at 300 rpm. BPR ratios were a) 30:1, b) 45:1, c) 60:1. Products were leached in 0.5 M HCl solution for 10 minutes.....	48
Figure 4.12. X-ray diagram for samples that were ball milled for 20 hours with 300 rpm and 30:1 BPR. a) Stoichiometric, b) 15 % Excess Mg addition.....	49

Figure 4.13. X-ray diagram of samples leached in 0.5 M HCl/water solution for 10 minutes a) Stoichiometric, b) 15% excess Mg addition.	50
Figure 4.14. X-ray diagram of samples ball milled for 20 hours with 300 rpm and 30:1 BPR. Products were leached in 0.5 M HCl/water solution for 10 minutes a) Reaction (4.1), b) Reaction (4.3) ...	52
Figure 4.15. Samples were ball milled with 300 rpm and 30:1 BPR for a) 20 hours, b) 30 hours, c) 60 hours	53
Figure 4.16. X-ray diagram for samples that were ball milled at 300 rpm and 30:1 BPR for a) 20 hours, b) 30 hours, c) 60 hours. Products of milling were leached with 0.5 M HCl/water solution for 10 minutes.....	54
Figure 4.17. X-ray diagram of samples ball milled with 300 rpm and 30:1 BPR for a) 10 hours, b) 15 hours.....	55
Figure 4.18. X-ray diagram of samples ball milled with 300 rpm and 30:1 BPR. Products of milling were leached with 0.5 M HCl/water solution for 10 minutes. Milling durations were a) 15 hours, b) 20 hours	56
Figure 4.19. X-ray pattern of Li_2B_9 reported by M. Panda at 100°K ⁽⁴⁾	57
Figure 4.20. Comparison of Li_2B_9 literature data ⁽⁴⁾ with the observed data. Powder was ball milled for 20 hours at 300 rpm with 30:1 BPR and leached in 0.5 HCl/water solution for 10minutes	57
Figure 4.21. X-ray diagram for samples that were ball milled for 20 hours with 300 rpm and 30:1 BPR. a) Reaction (4.1), b) Reaction (4.5).....	59
Figure 4.22. Samples were milled for 20 hours with 300 rpm and 30:1 BPR. Products were leached with 0.5 M HCl/water solution for 10 minutes. a) Reaction (4.1), b) Reaction (4.5).	60
Figure 4.23. X-ray diagram of samples that were ball milled for 20 hours with 300 rpm and 30:1 BPR. a) Li_2O as lithium source, b) $\text{Li}_2\text{B}_4\text{O}_7$ as lithium source.....	61

Figure 4.24. X-ray diagram of samples that were ball milled for 20 hours with 300 rpm and 30:1. Products of milling were leached in 0.5 M HCl solution for 10 minutes. a) Reaction (4.1), b) Reaction (4.6).....	62
Figure 4.25. Indexing of volume combustion synthesis product.....	64

CHAPTER 1

INTRODUCTION

Several different properties and applications of boron attract many scientists and engineers to study in boron chemistry. Boron compounds are widely used in different fields of industry, laundry products, fibreglass production, aerospace industry and glasses ⁽¹⁾. Boron has an atomic number of 5 and it is a semi-metallic element ⁽²⁾. Occurrence of boron in nature is in borate form and elemental boron is produced from commercial boron minerals such as tincal and colemanite. Turkey owns 72.2% of world boron reserves; it is followed by Russia with 8.5% and USA with 6.8% ⁽³⁾. Boron can combine with almost all elements in the periodic table to form borides ⁽⁴⁾.

Lithium is the lightest known metal and has many applications in industry, aerospace, batteries, nuclear power plants and drugs. Interesting properties of lithium make it available to use in such different application areas of industry. Location of lithium in periodic table is Group IA, alkali metals group. Main properties of lithium are, high electrochemical potential, light weight, high specific heat ⁽⁵⁾. It is highly reactive in elemental form and can react with water ⁽¹⁾.

Borides attracted much attention over the past fifty years because of their, crystal structure, physical properties and bonding situations ⁽⁴⁾. Binary metal borides have very interesting properties such as, high melting point,

high electrical conductivity, high oxidation and wear resistance ⁽⁶⁾. Lithium borides started to attract attention after 1966 with the publication of first lithium boride synthesis patent ⁽⁷⁾. Main investigation purposes of lithium boron compounds are related to their interesting chemical and physical properties which are the result of high mobility of lithium ⁽⁸⁾. Recent studies show that lithium borides have very promising properties in the area of high energy additives such as rocket fuels and hydrogen storage ^{(9) (10)}.

Aim of this study was to investigate the synthesis of lithium borides by mechanochemical synthesis. Syntheses of Li_3B_{14} , LiB_4 , Li_2B_6 and LiB_{13} were studied by using a planetary ball mill. Effect of milling parameters such as milling speed, ball to powder ratio (BPR) and milling duration were investigated. Starting materials were Li_2O , B_2O_3 and Mg and also $\text{Li}_2\text{B}_4\text{O}_7$ was used as lithium source instead of Li_2O . B_2O_3 was produced from H_3BO_3 by calcination. Experiments were conducted under argon atmosphere.

Fe and MgO were observed as other outputs of mechanochemical synthesis experiments. In order to clean these phases, powders were leached with dilute HCl/water solution for a pre-determined duration. Different leaching durations and concentrations were tested to find the optimum conditions. X-ray diffraction (XRD) and scanning electron microscopy (SEM) techniques were used for identification of phases.

Following this chapter, Chapter 2 will give brief information about production methods, structural properties of binary metal borides and previous studies related to lithium borides. Experimental procedure for preparation of reactant mixture, mechanochemical synthesis, leaching and analyses will be given in Chapter 3. Results of the experiments, data

obtained from analyses and discussions will be presented in Chapter 4. Conclusions obtained from discussions and observed data will be given in Chapter 5.

CHAPTER 2

LITERATURE REVIEW

2.1 Introduction

Alkali metal borides were first noticed at the beginning of nineteenth century ⁽¹¹⁾. Search for binary metal borides was accelerated during World War II. Undoubtedly, the war triggered the need for high-temperature materials which resulted in an increase in the investigations of metal borides. High temperature stability and chemical inertness of many metal borides made those subjects more attractive ⁽⁶⁾ ⁽¹²⁾. In this part, the past studies about borides, especially alkali metal borides and lithium borides, will be summarized.




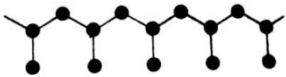
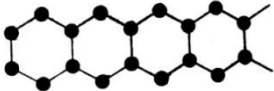
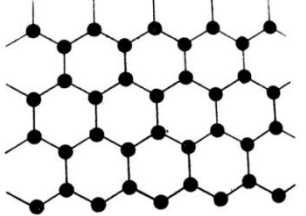
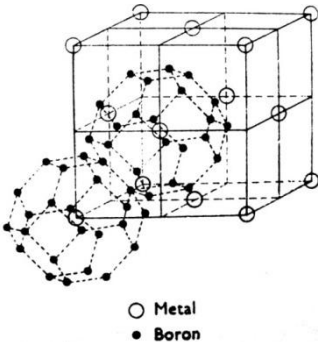
2.2 Classification of borides

Since boron is able to form compounds with most of the elements in periodic table, a system was necessary to classify the large group of boron compounds. Boron compounds that are formed with metals (M) are called true metal borides ⁽¹²⁾. Compound elements that have similar electronegativity as boron such as, carbon, silicon, nitrogen, phosphorus and arsenic were not classified as borides ⁽¹²⁾. Kiessling classified the boride compounds into four main groups ⁽⁶⁾ ⁽¹³⁾.

1. Borides formed of isolated boron atoms, such as M_4B and M_2B . Isolated pair formation increases when boron percent in the compound is increased ⁽⁶⁾ ⁽¹³⁾.
2. Borides formed of boron chains, such as MB , M_3B_4 ⁽⁶⁾ ⁽¹³⁾.
3. Borides formed of 2D boron atom nets, such as MB_2 , M_2B_5 ⁽⁶⁾ ⁽¹³⁾.
4. Borides formed of 3D boron frameworks, such as MB_4 , MB_6 , MB_{12} ⁽⁶⁾ ⁽¹³⁾.

Kiessling's structural classification is shown in Table 2.1. There are also other classification methods for borides such as, classification according to the location of metallic part in the periodic table ⁽⁶⁾ and classification according to boron content in the compound.

Table 2.1. Classification of borides according to Kiessling ⁽¹²⁾

Kiessling Group	Atomic Ratio	Examples	Structure
Isolated B Atoms	M_4B , M_3B M_2B	Mn_4B , Be_2B Ni_3B	
Pairs of B Atoms	M_3B_2	V_3B_2	
Single Chains	MB	FeB , NiB	
Branched Chains	$M_{11}B_8$	$Ru_{11}B_8$	
Double Chains	M_3B_4	Ta_3B_4 , Cr_3B_4	
Layer Networks	MB_2	TiB_2 , MgB_2 YB_2 , ReB_2	
3D Frameworks	MB_4 , MB_6 MB_{12}	CaB_6 , ZrB_{12} YB_{12}	

Classification of binary metal borides can also be made by referring to the parent metal group of periodic table. For example, boride compounds with group IA elements are called alkali metal borides or boride compounds with rare earth elements are called rare earth metal borides. Periodic classification of boron compounds is shown in Table 2.2. ^{(12) (14)}

Table 2.2. Periodic classification of borides ^{(12) (14)}

Period	I	II	III	IV	V	VI	VII	VIII
2	Li ₂ B ₆ Li ₃ B ₁₄	BeB ₁₂ BeB ₆						
3	Na ₃ B ₂₀ Na ₂ B ₂₉	MgB ₆ MgB ₄						
4	KB ₆	CaB ₆ CaB ₄	ScB ₁₂ ScB ₆	Ti ₃ B ₄ TiB ₂	VB ₂ V ₃ B ₂	CrB ₆ Cr ₃ B ₄	Mn ₂ B MnB ₂	Fe ₂ B FeB
5	RbB ₆	SrB ₆	YB ₆ YB ₁₂	ZrB ₂ ZrB ₁₂	Nb ₃ B ₂ NbB ₂	MoB ₄ MoB	Tc ₃ B TcB ₂	RuB ₂ Ru ₁₁ B ₈
6	CsB ₆	BaB ₆		HfB ₂	Ta ₂ B TaB ₂	WB ₄ WB	Re ₃ B ReB ₃	OsB ₂ Os ₂ B ₆
Lanthanides			LaB ₆ LaB ₄	CeB ₆	PrB ₆	NdB ₆		SmB ₆
Actinides				ThB ₄ ThB ₆		UB ₂ UB ₄		PuB ₆

2.3 Preparation of borides

There are several methods to produce binary metal borides. Synthesis process is chosen according to purpose of where the final product will be used. Generally, borides are synthesized from elements for research purposes. For industrial applications, oxides or hydrides of the reactants

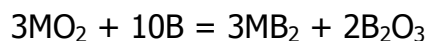
are used and production of them is accomplished with a reduction reaction. Following is a list of boride preparation methods ^{(6) (12)}:

a) Synthesis of boride from elemental reactants or boron and hydride of metal ^{(6) (12)}.



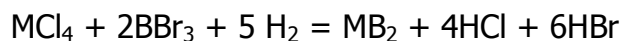
Using elemental reactants helps to obtain a boride with exact stoichiometric ratio. However, handling of elemental reactants causes other problems to be solved. Reaction between crucible material and reactants is another problem ^{(6) (12)}.

b) Metal oxide reduction by boron or a mixture of boron and carbon ^{(6) (12)}.



This process is used in laboratory applications. Elimination of B₂O₃ from output mixture is easy. However, using of elemental boron makes this process unsuitable for industrial applications ^{(6) (12)}.

c) Reduction of boron and metal halides with hydrogen ^{(6) (12)}.



This method is not suitable for Nb, Ta, Mo and W because of free metal deposition below boride formation temperature. This method is generally used for research purposes ^{(6) (12)}.

d) Reaction of boron halide with a metal or metal oxide and hydrogen. A wide range of borides can be synthesized with this method but yield is low and purity of the product is not sufficient ^{(6) (12)}.

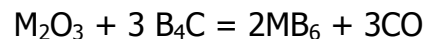
e) Preparation by electrolysis of fused-salt baths that contains metal oxide and boron oxide. Main problem in this method is the difficulty in separation of solid product from molten salt ^{(6) (12)}.

f) Metal oxide and boron oxide are reduced by carbothermic reaction ^{(6) (12)}.

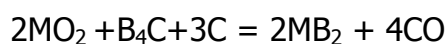


This method is suitable to produce metal borides in large quantities. It is not a preferred method to synthesize borides of metals which are remarkably volatile at reduction temperature ^{(6) (12)}.

g) Reaction between metal oxide and boron carbide ^{(6) (12)}.



Using B_4C instead of B_2O_3 solves the B_2O_3 volatilization problem and makes reaction faster. Additional free carbon may be used in this reaction as well ^{(6) (12)}.



h) Reaction of boron oxide with metals ^{(6) (12)}.

In this method a second elemental metal is used as reducing agent or metal part of the boride to be synthesized can be used as reducing agent. Synthesis of aluminium and magnesium borides can be given as examples for latter reaction. Acid insoluble metal oxides can cause purification problems in this process ^{(6) (12)}.

2.4 Lithium borides

Lithium-boron compounds were widely studied as candidate materials for batteries ⁽¹⁵⁾. Li-B system contains promising compounds. However structures have not yet been characterized completely ^{(8) (16)}. There are also other promising properties of lithium borides. LiBH₄ is a candidate compound for hydrogen storage because this compound can store theoretically 18.5 % mass hydrogen ⁽¹⁷⁾. It was proposed to synthesize LiBH₄ from its elements with ball milling by Çakanyıldırım and Gürü ⁽¹⁰⁾. Lithium and boron were reacted by ball milling to form LiB and then hydrogen applied to the samples in this study. Theoretical study of Zhao *et al.* showed that MB₁₀ (M=Li, Na, K) can be used as a ligand for novel nano-structured materials ⁽¹⁸⁾. Boron-lithium clusters were predicted to be used as additives to cryogenic hydrogen ^{(19) (20) (21) (22)}. LiB was also proposed as

a HEDM (High Energy Density Matter) ⁽²³⁾. Reactivity of lithium borides decreases as the lithium content in the compound decreases ⁽²⁴⁾ .

First prediction of alkali metal borides was made at the beginning of nineteenth century when elemental boron was tried to be produced by reduction of boron compounds with the help of alkali metals ⁽¹¹⁾. An alkali boride was proposed by Moissan in 1892 ⁽⁴⁾. It was confirmed by Kroll in 1918 and by Kahlenberg in 1925 ⁽⁴⁾. Naslain and Hagenmüller succeeded to produce KB_6 ⁽²⁵⁾ ⁽²⁶⁾, NaB_6 , NaB_{15} ⁽²⁷⁾ ⁽²⁸⁾ ⁽²⁹⁾. They also mentioned about existence of lithium borides. These compounds were reanalyzed in between 1998-2000 by Albert and Hoffman. It was proposed that actual composition of NaB_6 was Na_3B_{20} ⁽³⁰⁾ ⁽³¹⁾ ⁽³²⁾ and NaB_{15} was Na_2B_{29} ⁽³³⁾.

Lithium is extremely corrosive to metals and ceramics especially in liquid phase. This fact causes many problems when using conventional techniques for experiments ⁽³⁴⁾. In 1957, Markowskii *et al.* experimented several routes to synthesize lithium boride such as, the electrolysis of molten lithium borates, thermo-magnesium reduction of mixtures of $\text{Li}_2\text{O}+\text{B}_2\text{O}_3$, the reduction of B_2O_3 with lithium, reaction of boron with lithium hydride and direct synthesis from elements. Unfortunately, formation of lithium boride was not reported ⁽³⁵⁾.

First lithium boride LiB_4 was reported by Lipp in 1966 ⁽⁷⁾. It was proposed that synthesis of lithium boride was possible by reacting boron carbide and alkali metal (or alkali metal hydride). Temperature range for this process was between 500°C-1400°C and experiments were carried in a non-oxidizing atmosphere like Ar or H_2 . Cleaning of output material was done with mineral acid-water solution. In this patent, it was proposed that boron

rich alkali metal borides could be used as neutron absorbers and as additives for solid fuels.

$\text{LiB}_{10.85 \pm 0.35}$ was synthesized by Secrist ⁽³⁴⁾. Secrist studied compound formation in both lithium-carbon and lithium-boron systems. Lithium metal rod and β -rhombohedral boron were used in this study. Preparation of reactants was completed in a glove box and reaction experiments were done in an iron reaction capsule for 48 and 168 hours. Also, iron reaction capsule was closed with welding in argon atmosphere. Heating of samples was done in an electric furnace while iron reaction capsule was sealed with fused silica tubing. Secrist reported that after 9 atomic percent lithium, formation of lithium boride phase was observed.

Conduction-electron spin resonance in alkali hexaborides including LiB_6 was investigated by Rupp *et al.* in 1974 ⁽³⁶⁾. Existence of Li_2B was proposed by James and Devries in 1976 ⁽³⁷⁾. Li-B alloys were investigated as candidate material for thermal battery anodes. However, preparation of the alloy was very complicated due to the nature of elements and exothermic reaction between boron and lithium ⁽³⁸⁾. Crystal structure and composition of Li_5B_4 was investigated by Wang *et al.* in 1978 ⁽³⁹⁾. Preparation and synthesis of Li_5B_4 from its elements were completed under inert atmosphere in this study. They used crystalline boron and lithium. Reaction experiments were conducted in an iron crucible. They also used X-ray diffraction, neutron diffraction and nuclear magnetic resonance spectroscopy to characterize samples. Dalleck *et al.* studied lithium-boron alloy system with differential scanning calorimetry, metallography, X-Ray analysis in 1979. It was reported that Li_7B_6 was synthesized in this study ⁽⁴⁰⁾. Li-B alloys took attention as anode materials for thermal batteries ^{(41) (42)}.

Li_3B_{12} was theoretically predicted as a promising superconductor in 1993 by Gunji⁽⁴³⁾. B_{12} based materials have similarities to solid FCC C_{60} ⁽⁴⁴⁾ which is shown in Figure 2.1. Their theoretical study proposed that Li_3B_{12} was the most stable compound in Li_xB_{12} ($x=1,2,3,4$) group.

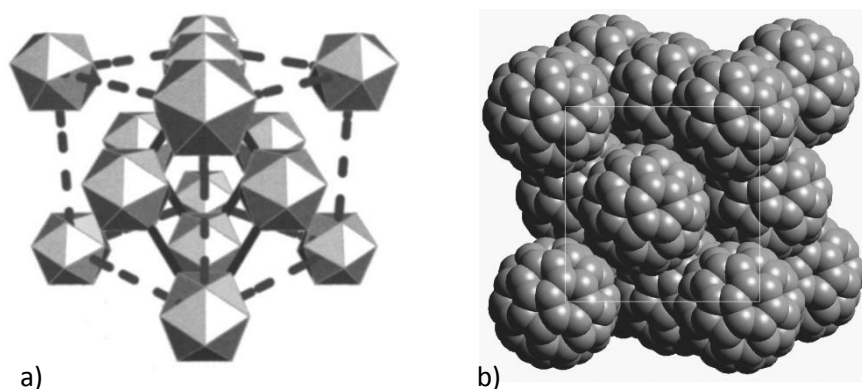


Figure 2.1. a) α -Rh Boron⁽⁴⁴⁾ b) FCC C_{60} ⁽⁴⁵⁾

Stability of lithium in α -rhombic boron was studied by Hayami *et al.* and it is proposed that Li at B_{12} structure can theoretically form⁽⁴⁶⁾. Similarities of boron compounds to carbon compounds were explained in detail by Jemmis and Jayasree⁽⁴⁷⁾. Their paper also pointed out structural similarity of C_{60} fullerene and B_{84} which are shown in Figure 2.2. Each vertex atom of B_{12} connected with a B_6 unit so that B_{84} is formed. Formation of B_{84} is shown in Figure 2.3.

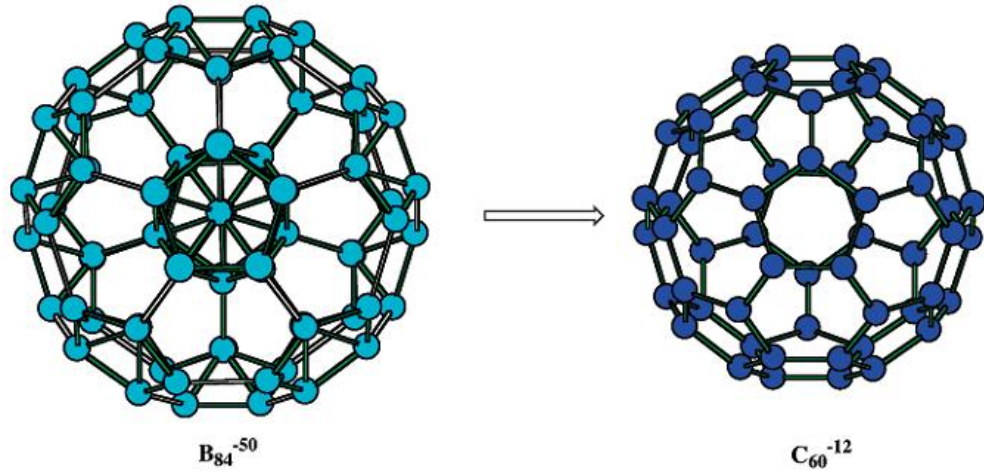


Figure 2.2. Structural similarity of β -rhombohedral boron and carbon ⁽⁴⁷⁾

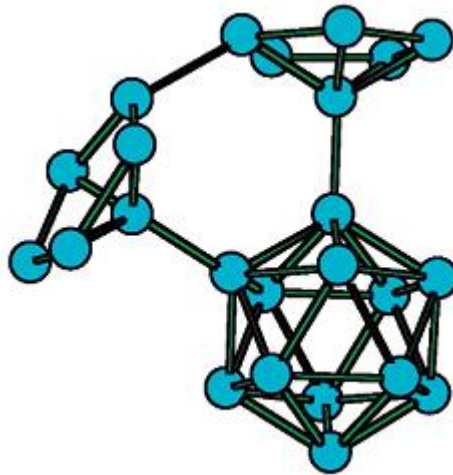


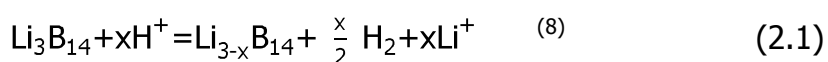
Figure 2.3. Formation of B_{84} . Two B_6 units connected to B_{12} icosahedra ⁽⁴⁷⁾

Experimentally synthesized LiB_{13} was reported to have β -rhombohedral structure by Kobayashi *et al.* ⁽⁴⁸⁾. Alkali metal doped β -rhombohedral has similar structure to potassium doped FCC C_{60} ⁽⁴⁹⁾. LiB_{13} was synthesized by using β -boron powder and lithium. They also reported that actual composition of this compound is $LiB_{12.9}$. Experiments were done on a

tantalum boat in a quartz tube. Heating temperature was 1000°C and experimental duration was 140 hours in this study ⁽⁴⁸⁾.

LiB₂ and LiB₁₀ were synthesized by Serebryakova *et al.* in 1994 ⁽⁵⁰⁾. Serebryakova reported that LiB₁₀ was resistant to corrosive materials. However, LiB₂ was a very unstable compound and decomposed even in weak acid solutions. LiB₃ was proposed by Meden ⁽¹⁵⁾ both theoretically and experimentally after a year.

Nesper and Mair succeeded to synthesize three new boride phases Li₃B₁₄, Li_{1.8}B₁₄ and Li₂B₆ ^{(8) (51)}. They used an improved experimental procedure to synthesize Li₃B₁₄, from β-rhombohedral boron and lithium. It is reported that usual container materials are weak against either boron or lithium. Because of that, they proposed to use a combination of containers. Nb ampoules were used as sealing container but niobium boride formation was inevitable. Therefore, reactants were placed into a Mo crucible and sealed with Nb ampoule which was enclosed by arc welding. They reported that Li₃B₁₄ forms compact polyhedral crystals. These are transparent red in transmission however; they look black under reflecting light. Nesper and his group also investigated physical properties, chemical properties and crystal structure of Li₃B₁₄. They reported that; the reaction of Li₃B₁₄ with H₂O is very slow. However, the reaction takes place more rapidly in strong acid solutions. Li₃B₁₄ reaction with protons is shown in reaction (2.1).



Reaction with H_2O resulted with the depopulation of lithium positions and that result turned the composition of the structure into $\text{Li}_{1.8}\text{B}_{14}$. Structural difference of $\text{Li}_{1.8}\text{B}_{14}$ and Li_3B_{14} was shown in Mair's study as in Figure 2.4.

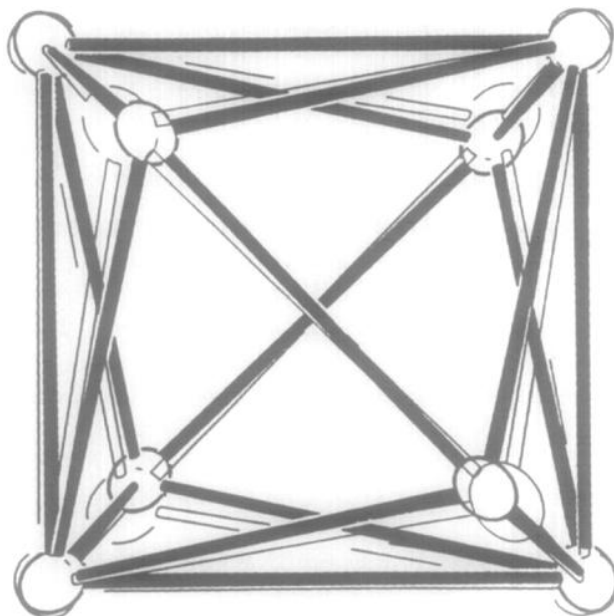


Figure 2.4. The structures of Li_3B_{14} boron cluster shown by black lines and the structure of $\text{Li}_{1.8}\text{B}_{14}$ cluster shown by white open lines ⁽⁸⁾

Crystal structure and morphology of LiB was investigated by Liu *et al.* in 2000 ⁽⁵²⁾. They reported that LiB compound is in fibre form and boron atoms in the compound are covalently bonded to each other. In the same year, another paper published by Nesper *et al.* confirmed the structure of LiB_x ($0.82 \leq x \leq 1$). Moreover, this study also showed that chains of boron atoms are surrounded by a lithium shell. Phase change of this compound at 150K was investigated in 2006 ⁽⁵³⁾. Phase diagram of B-Li system as shown in Figure 2.5, ⁽⁵⁴⁾ was given in Borgstedt's paper.

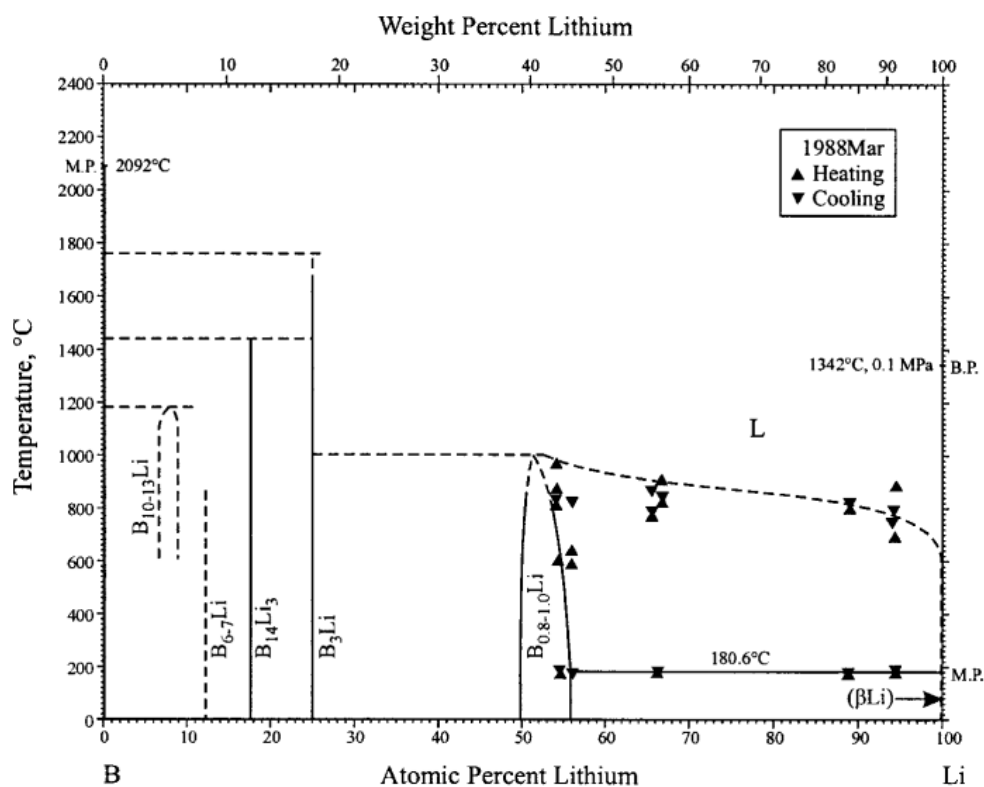


Figure 2.5. Phase diagram of B-Li system ⁽⁵⁴⁾

Lithium deficient LiB compound was also studied by Liu *et al* ⁽⁵⁵⁾. They investigated the crystal structure of the compound with X-ray diffraction by using three preparation methods. Hexagonal LiB compound was proposed as a new anode material for lithium ion batteries ⁽⁵⁶⁾.

Possibility of LiB to be used as anode material in lithium ion battery was investigated by Zhi-Jian *et al.* in 2005 ⁽⁵⁷⁾. Li_2B_9 was proposed by Schmitt *et al.* in 1997 ⁽⁵⁸⁾. A detailed study about alkali metal borides including LiB_{13} and Li_2B_9 was completed by M. Panda in 2006 ⁽⁴⁾. Main problems to synthesize lithium borides that are described in literature are;

1. Extreme sensitivity of lithium to impurities ⁽⁴⁾.
2. Reaction of starting materials with containers at high temperatures ⁽⁴⁾.
3. Melting point difference of lithium and boron ⁽⁴⁾.
4. Analyses of light elements like boron and lithium is difficult with conventional methods ⁽⁴⁾.
5. Multiphase synthesis of products ⁽⁴⁾.

In order to avoid these issues several precautions were taken in the past studies. Using glove box and different container combinations were some of them.

In this study, lithium boride compounds were synthesized from oxides of the reactant elements which are Li_2O and B_2O_3 to minimize the disadvantages of elemental reactants. It is reported that magnesiothermic reduction of these compounds does not yield a lithium boride compound ⁽³⁵⁾. Therefore, mechanochemical synthesis of lithium borides from Li_2O and B_2O_3 in presence of magnesium might give better results and so it was studied.

2.5 Mechanochemical synthesis

During thermal synthesis, solid-state reaction products form on the interface of reactants. Then, the product phase grows into the reactants by diffusion of reactant atoms. The product phase layer on the reactants hinders the rate of reaction. That is the main reason of heating the reactants to a reaction temperature. In mechanochemical synthesis, the contact area of the reactants is increased to a point that heating of the reactants is not necessary and reaction can take place at room temperature ⁽⁵⁹⁾.

Reduction of particle size during milling allows new generated surfaces to contact each other. Continuous mixing of powders increases the contact potential of those new surfaces. This mechanism eliminates the need for diffusion of atoms through the product phase ⁽⁵⁹⁾. Collision of balls to powder is shown in Figure 2.6. Two different types of kinetics are possible during mechanochemical synthesis ^{(60) (61) (62)}.

1. The synthesis reaction may take place gradually with a small transformation for each collision.
2. The synthesis reaction can take place with a self-propagating combustion reaction.

Self-propagating combustion reaction takes place at a critical milling time. At the critical time which is also called as ignition time, temperature of the container increases drastically. It is reported that only particle refinement occurs before combustion reaction ⁽⁶³⁾.

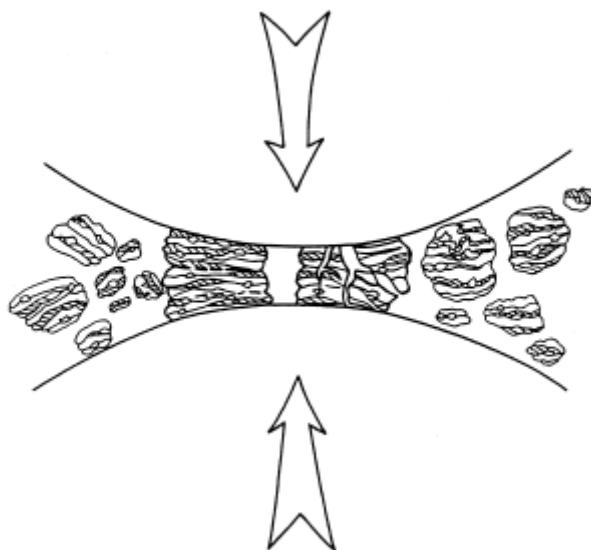


Figure 2.6. Ball to powder collision ⁽⁵⁹⁾

Close contact between reactants is an important parameter for mechanochemical process. This necessity is fulfilled in ductile-brittle reactant mixtures. Brittle reactants can easily mix into ductile matrix. This provides a close contact between reactants. In the case of brittle-brittle reactant mixtures, combustion reaction does not take place because close contact condition is not satisfied ⁽⁵⁹⁾.

There are important experimental parameters for mechanochemical synthesis. These parameters affect how the reaction takes place and efficiency of the process. These parameters are milling temperature, ball diameter, ball to powder ratio, process control agent and relative proportion of reactants ⁽⁵⁹⁾.

Milling temperature increases the reaction kinetics and decreases the process time unless a phase change occurs when temperature increased. Mc Cormick *et al.* reported that reduction process of TiCl_4 with Mg at room

temperature (20°C) was six times longer than when TiCl_4 is in solid state at -55°C ⁽⁵⁹⁾ ⁽⁶⁴⁾. This is was due to the fact that solid to solid collisions increased the process efficiency ⁽⁵⁹⁾.

It is reported in literature that an increase in the ball to powder ratio, decreases the process time. This is related to the fact that the rate of decrease of the particle size increases as ball to powder ratio increases ⁽⁵⁹⁾.

Process control agents that work as lubricants and surfactants are known to delay or suppress the combustion reaction between reactants. They are used to avoid the adverse effect of combustion reaction. Combustion reaction increases the particle size of the end product. Process control agent slows down reaction rate, hence the combustion reaction is inhibited ⁽⁵⁹⁾.

An increase in grinding ball diameter decreases ignition time of the process. Energy of collision increases when ball diameter increases so that process time decreases ⁽⁵⁹⁾.

CHAPTER 3

EXPERIMENTAL

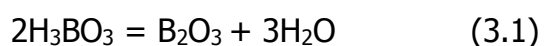
In this study, an alkali metal boride was aimed to be synthesized by mechanochemical process (MCP) in Lithium – Boron system. In this chapter, experimental techniques that were used during this study will be described. First, the input materials used in experiments will be explained. Then, the production method will be described. Finally, the characterization methods used for the final product will be given.

3.1 Input materials

Reactants used for mechanochemical synthesis of lithium borides were lithium oxide (Li_2O) by Alfa Aesar (99.5%) and boron oxide (B_2O_3). Boron oxide was produced from Merck boric acid (99.8%) by calcination. Details of the calcination process are explained in the following section.

3.1.1 Calcination of boric acid

Boron oxide was made from boric acid by calcination. Thermal decomposition reaction is shown in Reaction 3.1



Calcination process was conducted in a nickel crucible which had dimensions of; 50mm in height and 45mm in diameter. A pot furnace was used to heat the crucible to calcination temperature (Figure 3.1). The pot furnace was heated to 900°C. Boric acid was charged into nickel crucible and crucible was placed into the pot furnace. In order to let all charge to completely decompose, crucible was kept at this temperature for 45 minutes. After 45 minutes, all bubbles in liquid B_2O_3 left the charge, so the crucible was taken out of the furnace and immediately poured on to a stainless steel cooler plate. Solid boron oxide was removed from stainless steel plate when cooling was completed. In order to reduce the particle size, B_2O_3 pieces were crushed with hammer and ground into smaller pieces.

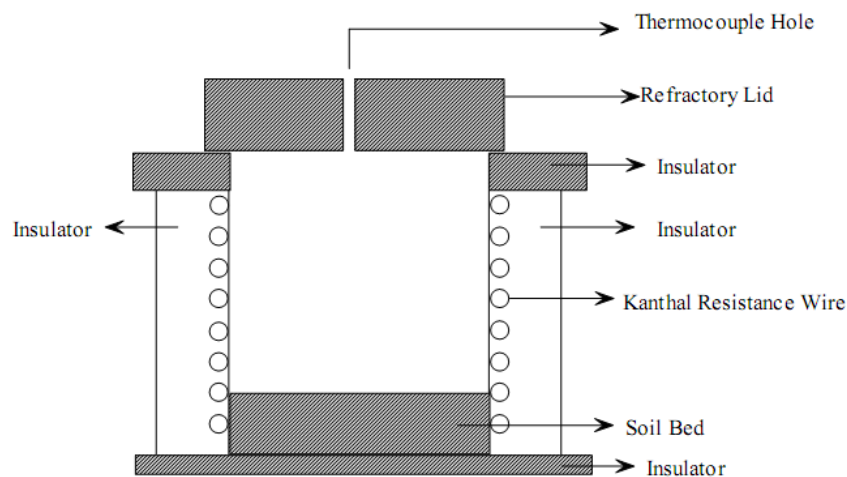


Figure 3.1.Pot furnace ⁽¹⁴⁾

3.1.2 Preparation of reactant mixture

Properties of reactant powders are given in Table 3.1. Reactant mixtures were prepared mainly according to reactions (3.2), (3.3), (3.4), (3.5), (3.6). Total mixture weight varied since ball to powder ratio was an essential variable for ball mill applications⁽⁵⁹⁾. In this study different ball to powder ratios were used in various experiments. After calcination process particle size of B₂O₃ was reduced to <5mm. It is observed that ball-milling of 8g B₂O₃ with 300 rpm (Revolutions Per Minute) for 20 minutes reduced the particle size of B₂O₃ to < 175µm.

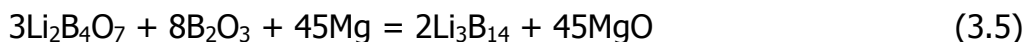
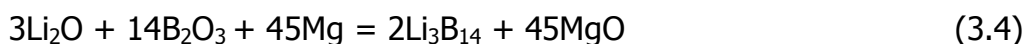


Table 3.1. Properties of powders

Powder	Purity	Company
Li ₂ O	99.5%	Alfa Aesar
Li ₂ B ₄ O ₇	---	Merck
Mg	99%	Riedel-de Haën
H ₃ BO ₃	99.8%	Merck

3.2 Ball milling

In this study, a stainless steel grinding jar and grinding balls were used for ball milling operation. Chemical analyses of ball mill equipment material are given in Table 3.2.

Table 3.2. Chemical analysis of grinding jar and balls ⁽⁶⁵⁾

Analysis	Grinding Jar	Grinding Balls
C	0.50 %	0.50 %
Fe	82.92 %	82.92 %
Cr	14.50 %	14.50 %
Si	1.00 %	1.00 %
Mn	1.00 %	1.00 %
P	0.045 %	0.045 %
S	0.030 %	0.030 %

Grinding jar had a volume of 250ml. Grinding balls had a diameter of 20mm. Top cover of the grinding jar had two gas inlets to modify the atmosphere of the experiment. The jar and balls are shown in Figure 3.2.



Figure 3.2. Milling equipment

Ball milling experiments were accomplished with a Retsch PM 100 planetary ball mill system. Device could operate between 100 and 650 rpm while loaded with grinding jar, sample and balls ⁽⁶⁶⁾. It is shown in Figure 3.3.



Figure 3.3. Retsch PM 100 planetary ball mill ⁽⁶⁶⁾

Working principle of planetary ball mill can be described as imitation of the planets⁽⁵⁹⁾. Grinding jar is placed in latching brackets which is located on a supporting disk. Grinding jar rotates around its own axis with the help of grinding jar fixture plate and latching brackets. The supporting plate rotates around its own axis in opposite direction to grinding jar when device is turned on. Grinding balls exert friction force while cycling on the inner surface of grinding jar. An impact force forms when the balls lift off and collide to the opposite wall of the jar⁽⁵⁹⁾. Particle size of the sample in the jar decreases as a result of these friction and impact forces. Figure 3.4 shows the motion of grinding balls in the jar.

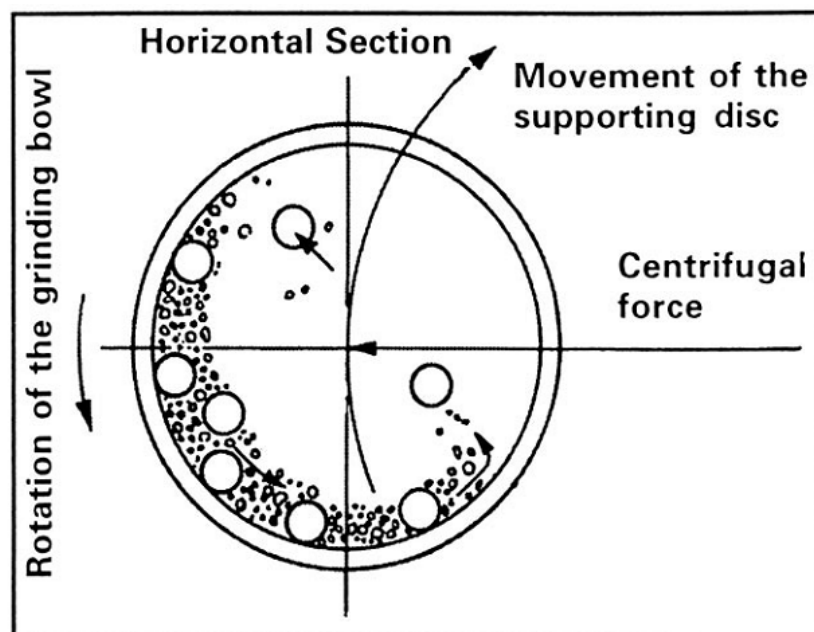


Figure 3.4. Motions of balls in planetary ball mill jar⁽⁵⁹⁾

Before starting the milling operation, reactant mixture was prepared and put into grinding jar with 8 balls. Then, top cover of the jar was closed and tightened with locking arrangement. After tightening of all three bolts and

nuts equally, air inside the jar was evacuated with a vacuum pump for 10 minutes. The jar was flushed with argon immediately after evacuation, in order to provide an inert atmosphere during the experiment. The jar was weighed and placed into the ball mill. After clamps were locked, counterweight on the support plate was balanced with the jar. Final view of the ball mill is shown in Figure 3.5.

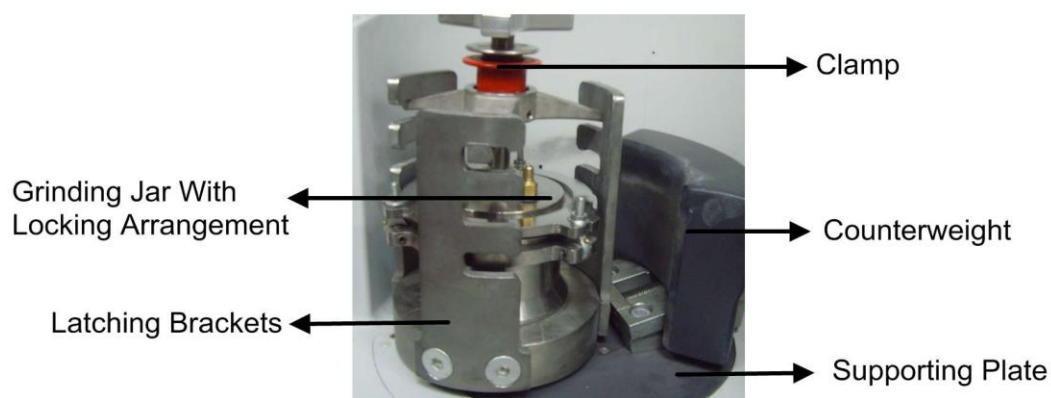


Figure 3.5. Jar in the ball mill

Finally, milling parameters for the experiment were set by using graphic display of the ball mill.

3.3 Ball Milling for Mechanochemical Process

Ball milling operation for mechanochemical synthesis was done with the equipment and procedure explained in Section 3.2. Experimental milling parameters that were used in this study are rotational speed, ball to

powder ratio (BPR), and milling duration. Variables are given in Tables 3.3 and 3.4.

Table 3.3. Ball mill parameters

Parameter	Value				
BPR	1/30	1/45	1/60		
Rotational Speed (RPM)	200	250	300	400	
TIME (Hours)	10	15	20	30	60
Balls	8 Pieces – 20mm Ø, Stainless Steel				
Medium	Dry Ball Milling				
Atmosphere	Argon				

Table 3.4. Experimental parameters used

No	Rotational Speed (RPM)	Duration (Hours)	BPR
1	200	20	1/30
2	250	20	1/30
3	300	20	1/30
4	400	20	1/30
5	300	10	1/30
6	300	15	1/30
7	300	20	1/30
8	300	30	1/30
9	300	60	1/30
10	300	20	1/45
11	300	20	1/60

All ball milling experiments were completed with 30 minutes intervals and 1 minute break time between intervals. The grinding jar started to rotate in the reverse direction when 1 minute break was completed.

3.4 Leaching process

Leaching is a chemical process of removing a solid from a mixture of solids by dissolving one or more of the solids in the mixture ⁽⁶⁷⁾. Type of leaching solvent, concentration of solvent, duration of process and process temperature are the main parameters that affect the final concentration of the recovered part. Main principle to recover the desired part of the batch is to use a leaching agent in which the desired part is insoluble or slightly soluble. However, unwanted part of the batch should be soluble ⁽⁶⁸⁾.

Leaching was applied as a final process, in order to remove the unwanted experimental impurities and process outputs such as Fe and MgO. Iron in the final mixture resulted from mechanical removal of stainless steel particles from jar and ball surface during milling. The main aim of leaching process was to obtain a relatively pure product and also remove the other reaction outputs that mask the analyses of the product.

MgO is soluble in acids and ammonium chloride solutions ⁽⁶⁹⁾. In order to dissolve MgO, HCl solution diluted with water was used as leaching reagent. 37% HCl (Riedel-de Haën) acid solution was used in the leaching process. HCl has a molecular weight and density 36.46g/mol and 1.19 g/ml, respectively. Molarity calculation of commercial HCl was as follows:

$$\text{Molarity of HCl} = \frac{37\text{g HCl}}{100\text{g}} \times \frac{1\text{mol}}{36.46\text{ g}} \times 1.19 \frac{\text{g}}{\text{ml}} \times 1000 \frac{\text{ml}}{\text{l}} = 12.076 \frac{\text{mol}}{\text{l}}$$

In order to determine the critical saturation of the leaching solution, solutions with different molarities were prepared such as 0.375M, 0.5M, 1M, 2M HCl. Preparation of 1M leaching solution was completed by mixing HCl with deionised water according to the following calculation;

$$\frac{1\text{ mol}}{12.076\text{ mol/l}} \times 1000 = 82.8\text{ml of 37\% HCl}$$

82.8ml of 37% HCl was mixed with 917.2ml of deionised water. Mixing ratio of powder to HCl solution was 1g/100ml in all experiments.

Mixing of powder and leaching solution was done with an Ikamag RCT magnetic stirrer and a magnetic stirring bar (Figure 3.6). The powder was weighed and leaching solution was measured according to slurry density ratio. The leaching solution was poured into a beaker and beaker was put on the magnetic stirrer. After that, the magnetic stirrer bar was put into beaker. Then, the prepared powder was added on to leaching solution and stirrer was started. All leaching operations were completed at room temperature.

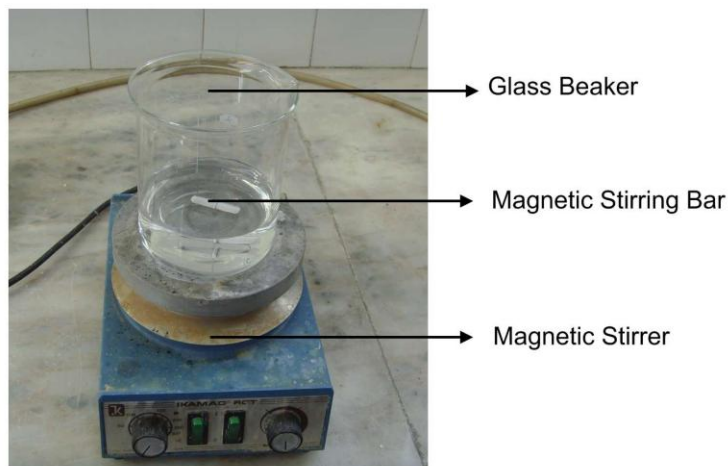


Figure 3.6. Leaching equipment

After stirring of slurry for a predetermined time, glass beaker was taken from magnetic stirrer for filtration of powders. Filtration was applied in order to separate insoluble solid, from liquid. Whatman 110mm Ø Grade 42 filter paper was used for filtration. Filter paper was placed on funnel and liquid was separated from solid by the help of a vacuum pump. Filtration equipment is shown in Figure 3.7. Vacuum pump was connected to the flask. After pouring the mixture onto the filter paper very slowly to avoid splashing and loss, vacuum pump was started. Wet solid residue was the product of the experiment. Filtration process was completed after all the solids were separated from liquid part.

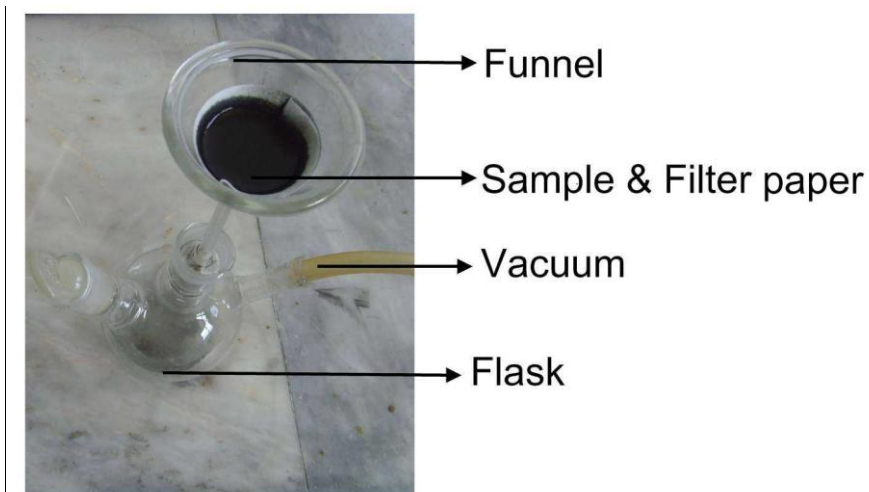


Figure 3.7. Filtration equipment

Wet solid sample was dried in a drying oven after washing which was set at 105 °C. After 20mins of drying time, the filter paper with powder material was weighed and experimental product weight was calculated. Finally, coated powder on the filter paper was removed by scraping.

3.5 Analysis Methods

A Rigaku Multiflex Powder X-ray diffractometer available at Metallurgical and Materials Engineering Department of METU was used for analysis of the samples. (Figure 3.8). Samples were analysed with Cu-K α radiation. Scanning rate was 2°/min and steps were 0.02°. 2 θ Angle range was 10-80° for most of the samples. Phase identification was completed with the help of qualitative analysis software tools such as smoothing, background subtraction, K α 2 elimination.

A Jeol JSM 6400 scanning electron microscope (SEM) located at Metallurgical and Materials Engineering Department of METU was used for the examination of particle morphology of samples. (Figure 3.9) Also elemental analysis of the samples was done with NORAN System 6 X – Ray Microanalysis System.



Figure 3.8. Rigaku Multiflex Powder X-ray diffractometer ⁽¹⁴⁾



Figure 3.9. Jeol JSM 6400 scanning electron microscope ⁽¹⁴⁾

CHAPTER 4

RESULTS AND DISCUSSION

4.1 Introduction

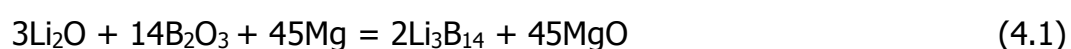
The aim of this study was to investigate synthesis of lithium borides from oxides by mechanochemical production. Li_3B_{14} (trilithium tetradecaboride) structure was observed in synthesis products. Synthesis experiments were also conducted for other lithium borides by using Li_3B_{14} structure as reference. This chapter explains the results and observations obtained from lithium boride synthesis experiments. Mechanochemical synthesis experiments of lithium borides were completed according to the experimental procedure that is given in Chapter 3. In order to understand the synthesis reaction properties, experiments were done with different parameters. These parameters were ball-mill speed, ball to powder weight ratio, effect of excess magnesium addition, Li to B ratio and leaching conditions. First of all, ball milling parameters were investigated.

4.2 Effect of ball mill speed

There could be two different types of mechanochemical reduction reaction; gradual reaction of reactants or self-propagating combustion reaction ⁽⁵⁹⁾. Ball milling parameters could affect the type of reduction reaction as explained in Chapter 2. In order to understand the effects of ball milling

parameters on lithium boride synthesis, different parameters were experimented.

Rotational speed was one of the most important parameters for mechanochemical synthesis in planetary ball mill. In order to understand the effects of rotational speed on synthesis of lithium borides, a sample was prepared according to reaction (4.1).



Sample mixtures prepared according to the above reaction were ball milled for 20 hours with 30:1 BPR (Ball to Powder Ratio). The speed parameters tested were 200, 250, 300 and 400 rpm. It was observed that the reaction did not take place at 200 and 250 rpm. Results of the experiments are shown in Figure 4.1.

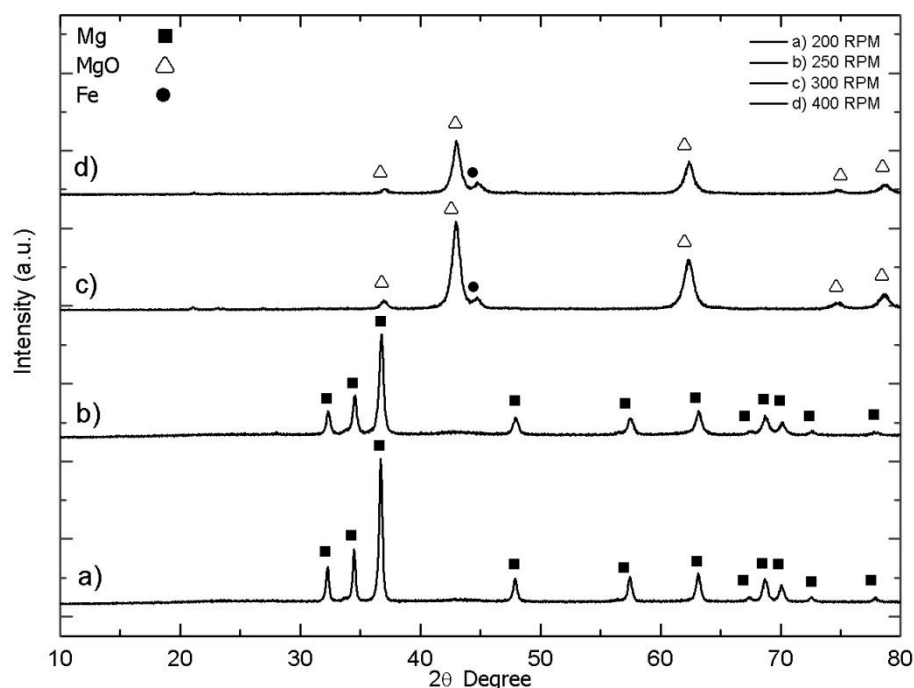


Figure 4.1. X-Ray Diagram for samples ball milled for 20 hours with 30:1 BPR a) 200 rpm, b) 250 rpm, c) 300 rpm, d) 400 rpm.

It was observed that low speeds of milling such as 200 and 250 rpm did not supply enough energy for the reaction to happen. X-ray diffraction pattern of the sample showed only magnesium peaks. Other reactants, B_2O_3 and Li_2O were not observed on diffractograms (a) and (b). Absence of B_2O_3 peaks could be explained by amorphous structure of the powder which was the result of rapid cooling after calcination of H_3BO_3 . Structure of B_2O_3 after calcination is shown in Figure 4.2. The reason for the absence of Li_2O peaks could be due to the relatively low weight percent of Li_2O . Reaction started to take place at 300 rpm, Fe and MgO peaks were observed on diffractograms of (c) and (d). Products of 300 and 400 rpm were leached with 0.5M HCl/water solution for 10 minutes. Results of the experiments for 300 and 400 rpm are shown in Figure 4.3

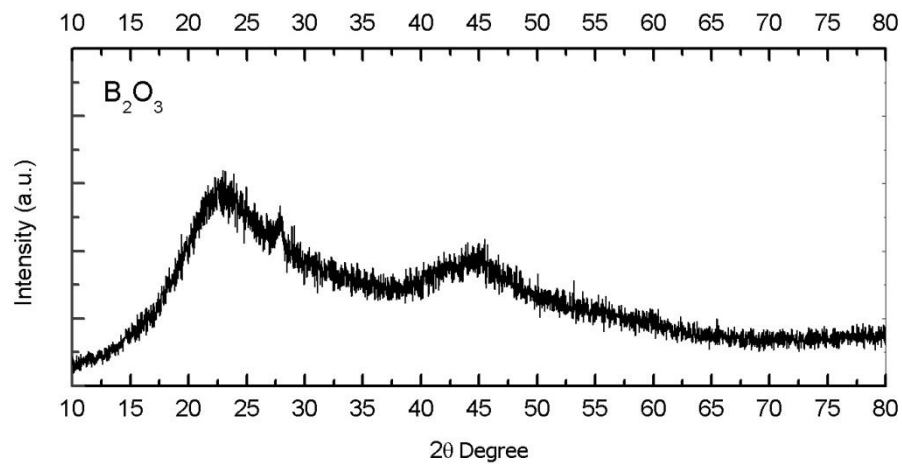


Figure 4.2. X-ray diagram of B_2O_3 after calcination of H_3BO_3 .

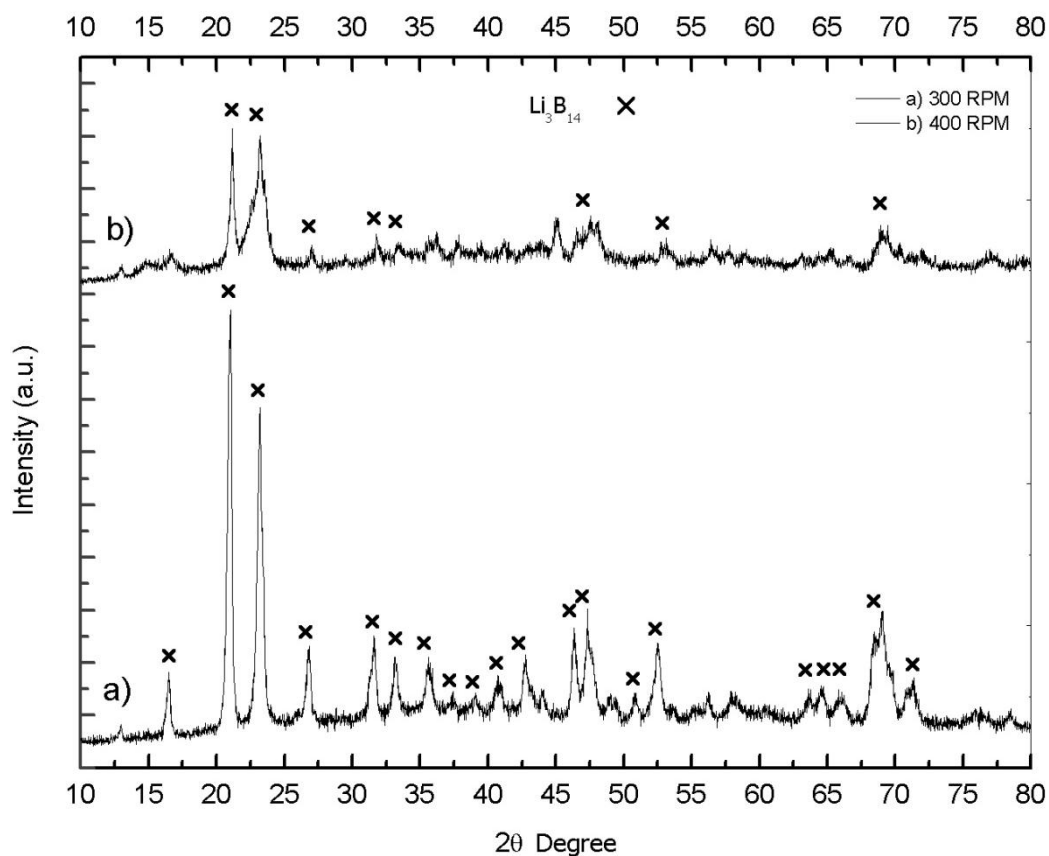


Figure 4.3. X-Ray Diagram for samples ball milled for 20 hours with 30:1 BPR a) 300 rpm, b) 400 rpm. Both samples were leached with 0.5 M HCl solution for 10 minutes

Figure 4.3 shows that reaction products of 300 and 400 rpm were found to contain Li_3B_{14} . Peaks of Li_3B_{14} in sample (b) were broadened which was the result of particle size reduction for 400 rpm. Broadening of the peaks is shown in Figure 4.4.

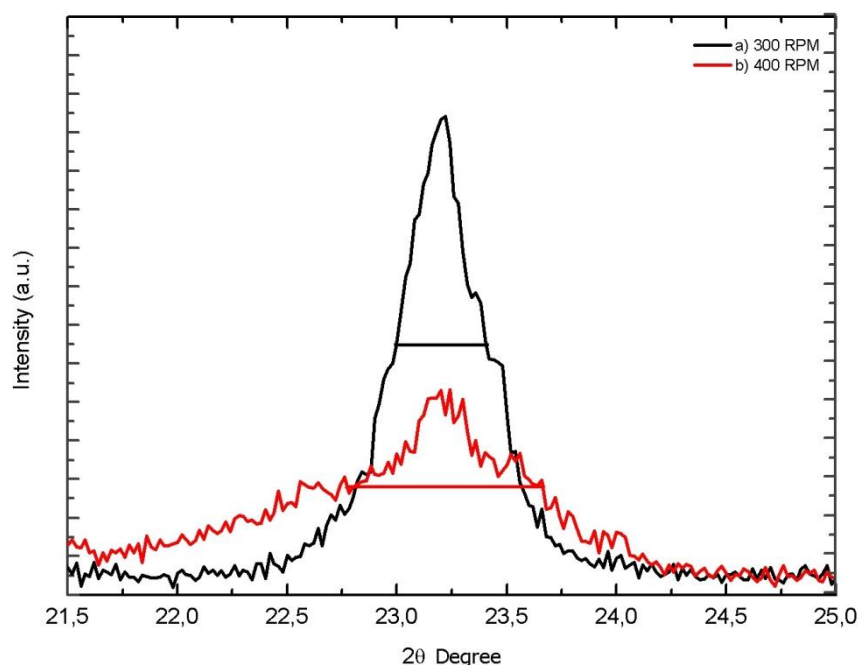
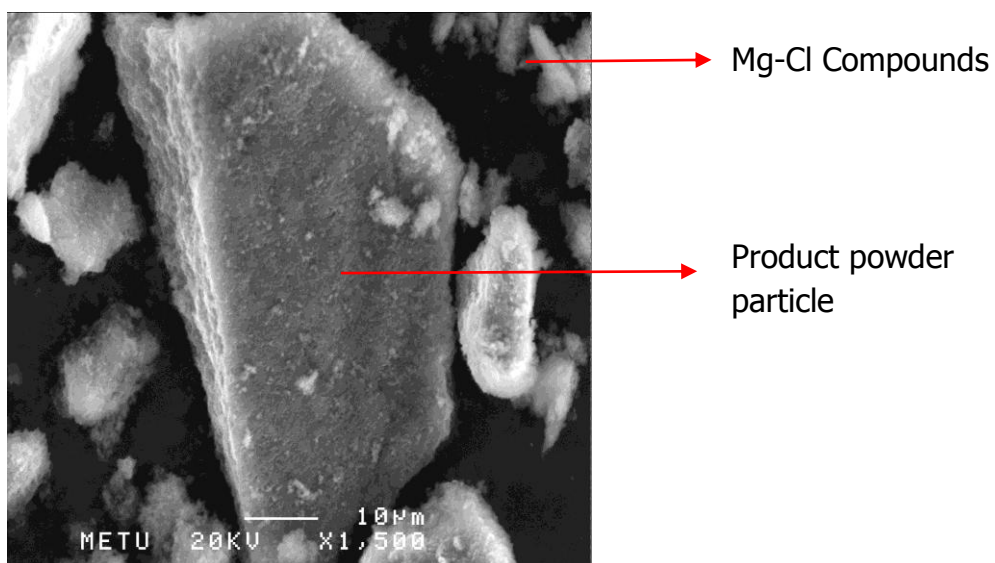
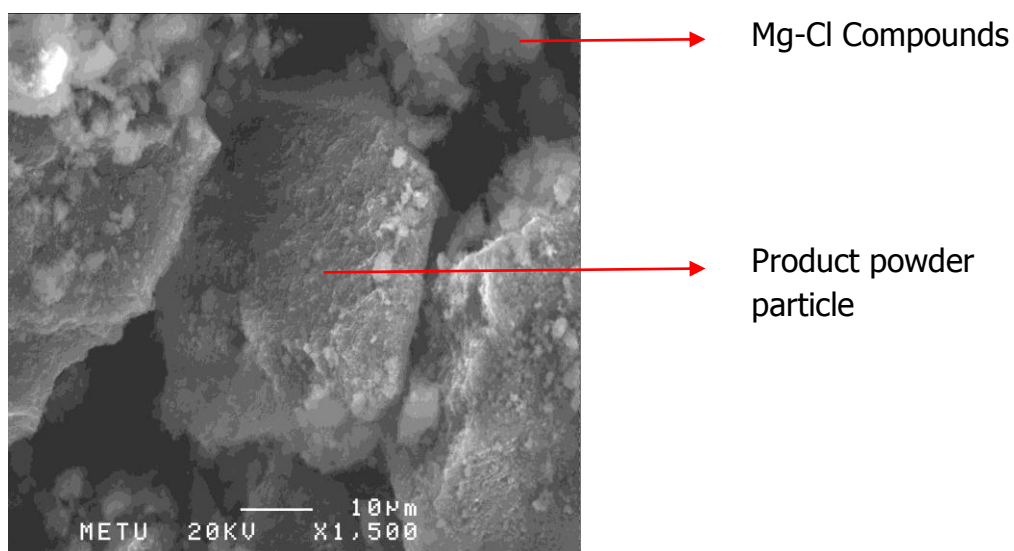


Figure 4.4. X-Ray Diagram for samples ball milled for 20 hours with 30:1 BPR a) 300 rpm, b) 400 rpm. Both samples were leached with 0.5 M HCl solution for 10 minutes

Red and black horizontal lines intersect peaks at half maximum. Width of the red line is longer than the black which indicates that particle size of the sample with 400 rpm is smaller than that of sample with 300 rpm. Increasing the milling speed resulted in a distortion of Li_3B_{14} pattern. Therefore, it was decided that 300 rpm was a satisfactory parameter for ball milling. Also, product weight of the sample was measured as 0.28g which indicated that efficiency of the process for sample (a) was 87.8% when compared to theoretical value.



(a)



(b)

Figure 4.5. SEM Micrographs for samples ball milled for 20 hours with 30:1 BPR and leached in 0.5 M HCl solution for 10 minutes, a) 300 rpm, b) 400 rpm

Figure 4.5 shows particle morphologies of the powders that were synthesized with 300 and 400 rpm. Powders in these micrographs were not coated with gold for EDS. The reason for this was that the product

powders had sufficient conductivity to carry out such analysis. EDS of powders indicated the presence of a small amount of Mg and Cl elements as well. Cotton like white particles in the micrographs were thought to be Mg-Cl compounds which remained in the powder because of precipitation during drying of filter paper.

4.3 Effect of leaching parameters

Leaching parameters were very important to recover the final product with minimum loss and as pure as possible. In the case of lithium boride, it is known that, the stability of boride in acid solutions decreases as the lithium percent in the compound is increased. Boron rich compounds such as LiB_{10} were reported to be resistant to acidic media ⁽⁵⁰⁾. Samples that were analysed by XRD before leaching did not give much information about final product, because high intensity of MgO peaks prevented the detection of other peaks as seen in Figure 4.6.

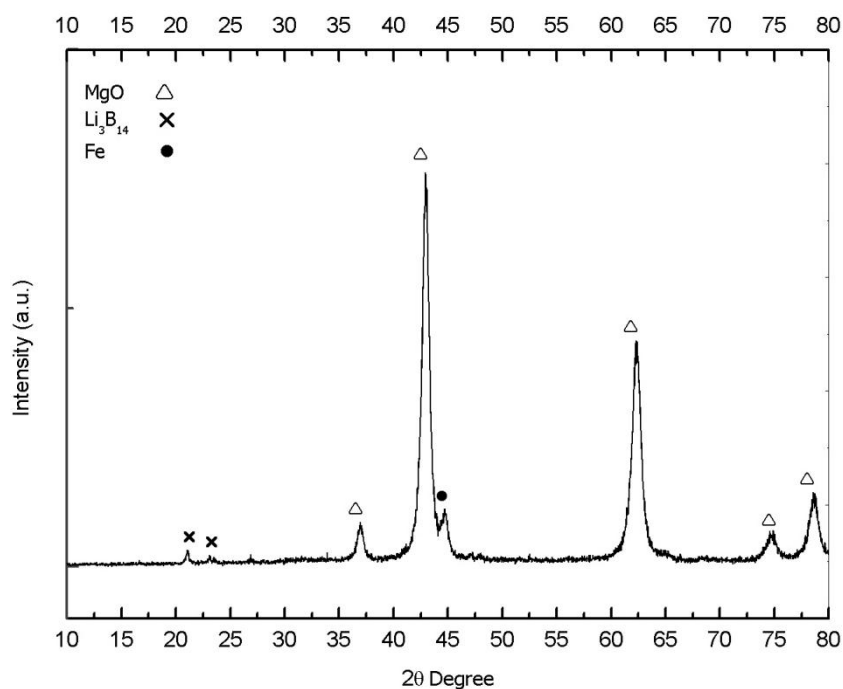


Figure 4.6. X-Ray Diagram for a sample ball milled for 20 hours with 30:1 BPR and 300 rpm

As seen on Figure 4.6, MgO peaks were extremely dominant over Li_3B_{14} peaks. Figure 4.6 also shows iron peaks in the diffractogram. Iron contamination of the powder was the result of wear of the milling equipment during process.

In order to find out the optimum parameters for leaching, initially the critical concentration of the leaching solution should be determined. For this purpose, samples were ball milled for 20 hours with 300 rpm and 30:1 BPR. Composition of reactant mixture was prepared according to the reaction (4.1).

After milling, the samples were leached with 0.375 M, 0.5 M, 1 M and 2 M HCl/water solutions, respectively for 10 minutes according to the

procedure explained in Chapter 3. XRD diagrams of the samples are shown in Figure 4.7. XRD analysis of the 2 M sample could not be done because 2 M HCl/water solution made the filter paper very brittle which did not allow scraping of residual powder. Therefore, 2 M and above concentrations were not used for the latter studies because of the experimental difficulty.

It was also observed that during leaching iron separated from leach slurry mechanically by gathering on magnetic stirrer.

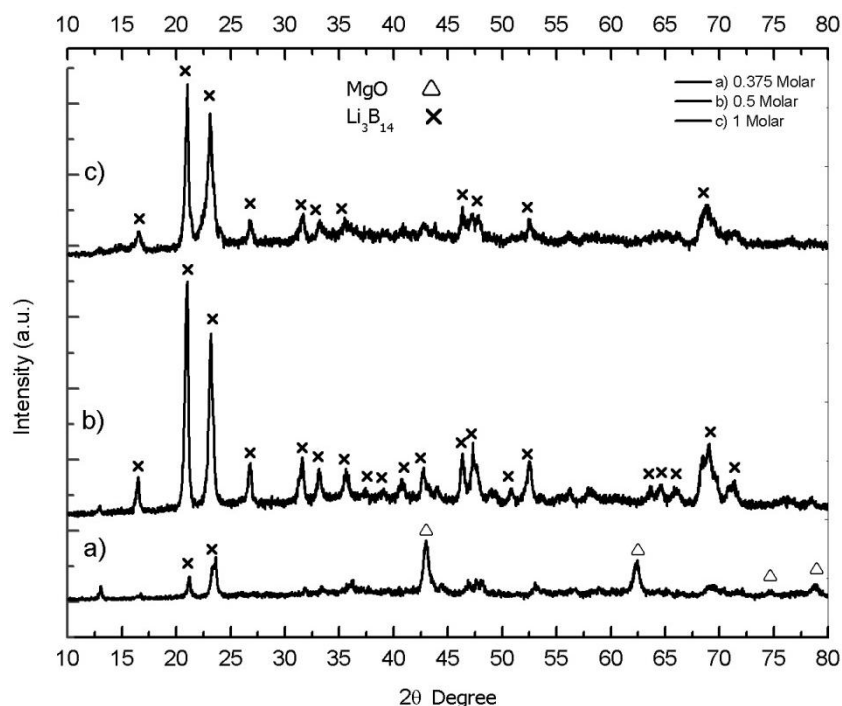
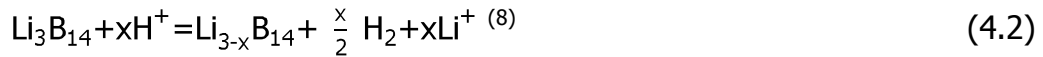


Figure 4.7. X-ray diagram for samples that were ball milled for 20 hours with 300 rpm and 30:1 BPR. Products of ball mill were leached with a) 0.375 M, b) 0.5 M, c) 1 M, HCl solutions for 10 minutes

As seen in Figure 4.7 (a), 0.375 M HCl/water solution was not strong enough to leach all MgO in the sample. Intensity of MgO peaks was

reduced when the concentration of HCl in solution was increased and at 0.5 M HCl characteristic peaks of MgO particles completely disappeared.

Peaks of sample (b) and (c) in Figure 4.7 were indexed as Li_3B_{14} . Further increase in HCl concentration reduced the intensity of the peaks. Lithium in the Li_3B_{14} structure could be lost to leaching solution because of reaction (4.2) which was reported by Nesper *et al.* ⁽⁸⁾. They also reported that reaction (4.2) and lithium loss in the Li_3B_{14} structure by other means resulted in nearly identical X-ray patterns in $\text{Li}_{3-x}\text{B}_{14}$ for $x \leq 1.7$ ⁽⁸⁾. Therefore, the exact indexing of lithium boride in this range was not possible much with X-ray diffractogram analyses. However, Li_3B_{14} pattern in the diffractogram could be stated as an indication of the existence of B_{14} -frame ⁽⁸⁾.



Therefore, HCl concentration for leaching solutions was chosen as 0.5 M to reduce the risk of lithium loss.

Leaching duration of the process was another parameter to be determined. In order to understand the effect of leaching duration on final product, the reactant mixture was prepared according to reaction (4.1). Samples were ball milled for 20 hours with 300 rpm and 30:1 BPR. Leaching experiments were conducted with 0.5 M HCl/water solution for 10-30-60 minutes. Results are shown in Figure 4.8.

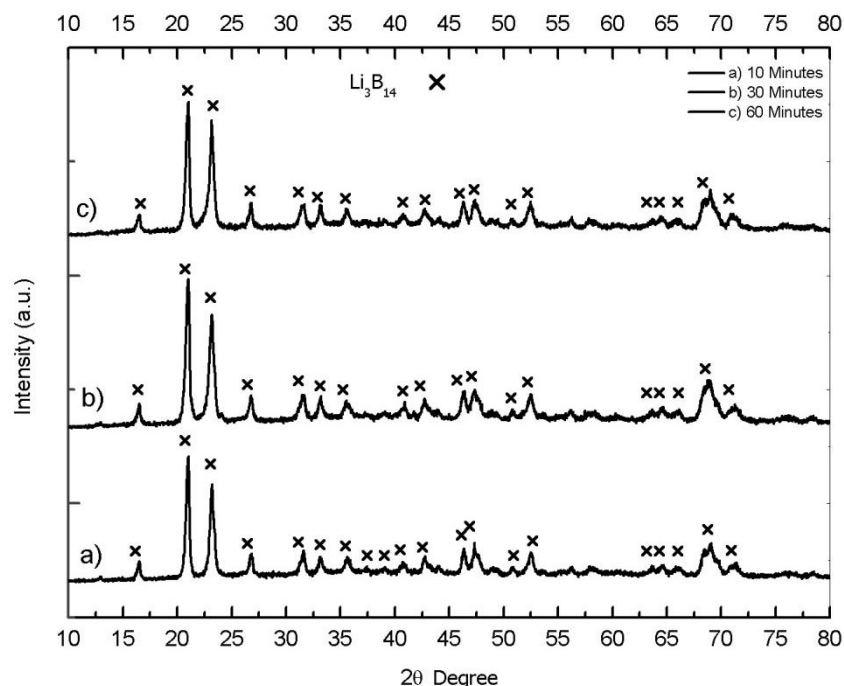


Figure 4.8. X-ray diagram for samples that were ball milled for 20 hours with 300 rpm and 30:1 BPR. Products of ball mill were leached with 0.5 HCl/water solutions for a) 10 minutes, b) 30 minutes and c) 60 minutes

As seen in Figure 4.8 the leaching duration had no significant effect on final product phase. Even though, Li_3B_{14} kept its structural pattern at least up to one hour, the leaching duration was chosen as 10 minutes to reduce the possibility of lithium loss.

4.4 Effect of ball to powder weight ratio

Ball to powder weight ratio was another parameter investigated that increased energy applied to powders when the ratio is increased. Figure 4.9 shows the effect of ball to powder ratio prior to leaching. Samples that were prepared according to reaction (4.1) were produced by ball milling for 20 hours at 300 rpm with different BPR ratios.

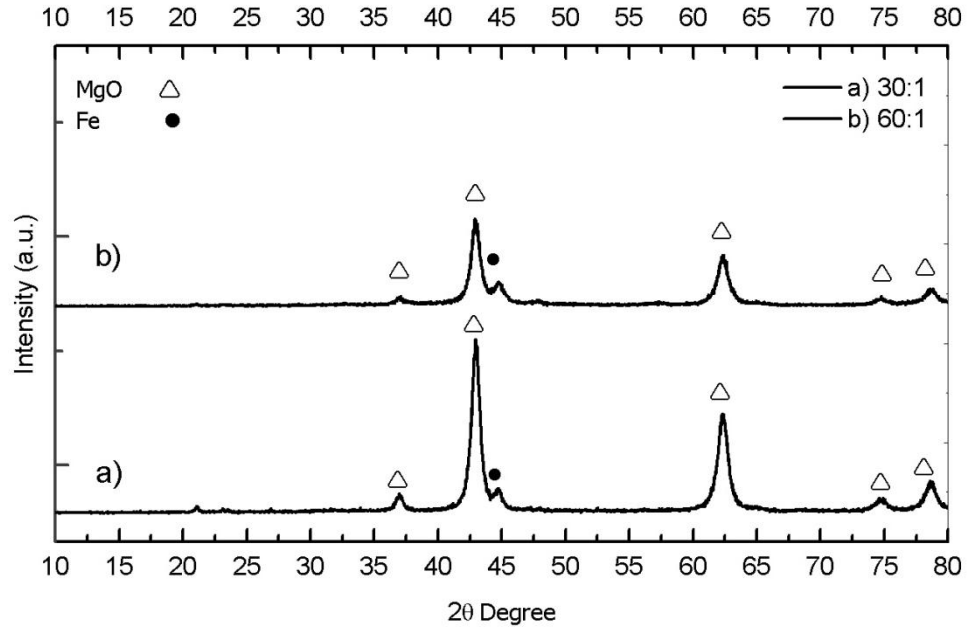


Figure 4.9. X-ray diagram for samples that were ball milled for 20 hours at 300 rpm with a) 30:1 and b) 60:1 BPR

Figure 4.9 shows a decrease in the intensity of the peaks when BPR increased and also iron contamination exists in both samples. Particle size refinement and lattice strain increase cause broadening and consequently a decrease in peak heights during ball milling ⁽⁵⁹⁾. Therefore, it can be commented that an increase in BPR, decreases the particle size of the product.

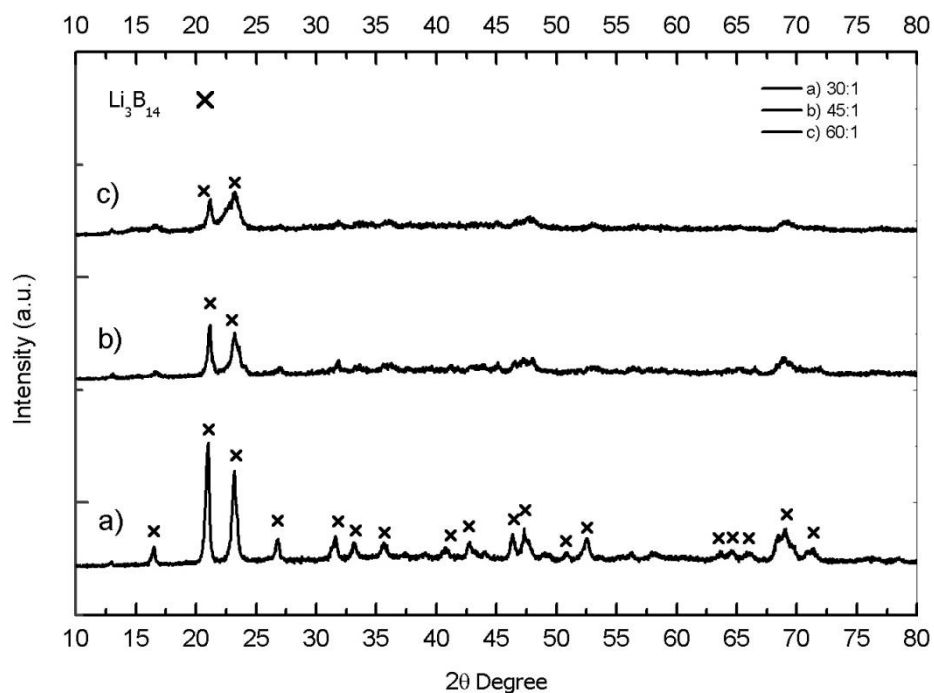


Figure 4.10. X-ray diagram for sample ball milled for 20 hours at 300 rpm. BPR ratios were a) 30:1, b) 45:1, c) 60:1. Products were leached in 0.5 M HCl solution for 10 minutes

Figure 4.10 shows products of milling that were leached in 0.5 M HCl/water solution for 10 minutes. Similar to rotational speed, an increase in ball to powder weight ratio resulted in broadening of peaks and a consequent decrease in the peak heights. Broadening of the peaks can be observed more clearly in Figure 4.11. BPR of 30:1 was satisfactory for both indexing of the product and detection of other possible phases.

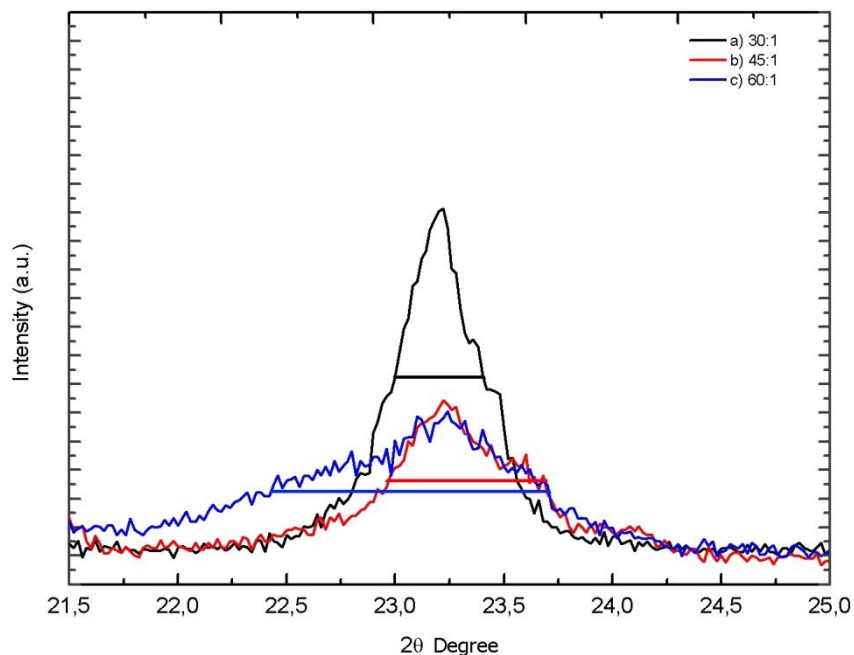


Figure 4.11. X-ray diagram for sample ball milled for 20 hours at 300 rpm. BPR ratios were a) 30:1, b) 45:1, c) 60:1. Products were leached in 0.5 M HCl solution for 10 minutes

Effect of BPR can be seen more clearly in Figure 4.11. In this figure, black, red and blue horizontal lines intersect peaks at half maximum intensity. The longest line is blue which indicates that the crystal size of sample (c) is smaller than the other samples. Also red line is longer than black which means the crystal size of sample (b) is smaller than (a).

4.5 Effect of excess magnesium

Effect of excess magnesium addition was investigated for 15% and 30% excess magnesium amount. Samples were prepared according to the composition of reaction (4.1) with 15% and 30% excess magnesium. Reactant mixtures were ball milled for 20 hours with 300 rpm and 30:1

BPR. It was observed that reaction did not take place for sample with 30% excess magnesium. Particle refinement of ductile particles such as magnesium is different when compared to brittle particles. Ductile particles absorb energy supplied in to the system during work hardening so that critical milling time for ignition increases ⁽⁵⁹⁾. It is commented that an increase in the magnesium amount in the sample, resulted with an increase in the critical milling time. Therefore, reaction did not take place for sample with 30% excess magnesium. Results of samples with 15% excess magnesium before leaching are given together with the stoichiometric magnesium addition sample in Figure 4.12.

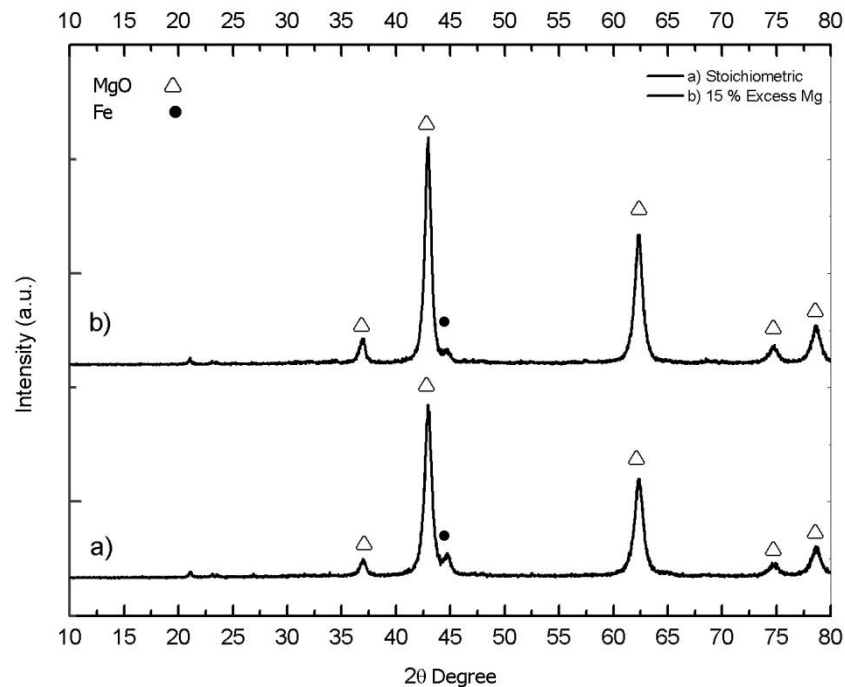


Figure 4.12. X-ray diagram for samples that were ball milled for 20 hours with 300 rpm and 30:1 BPR. a) Stoichiometric, b) 15 % Excess Mg addition

Figure 4.12 shows an increase in the peak intensity values of sample which has 15% excess magnesium when compared to the stoichiometric counterpart. Higher intensity value meant an increase in the amount of

MgO produced and an increase in the relative amount of MgO. BPR was the same for both samples so reactant mixtures were prepared with the same weight. Therefore, the relative amount of magnesium in the mixture was increased while other reactants Li_2O and B_2O_3 were decreased. An increase in the magnesium amount of reactant mixture also increased the MgO output of the process and consequently height of MgO peaks.

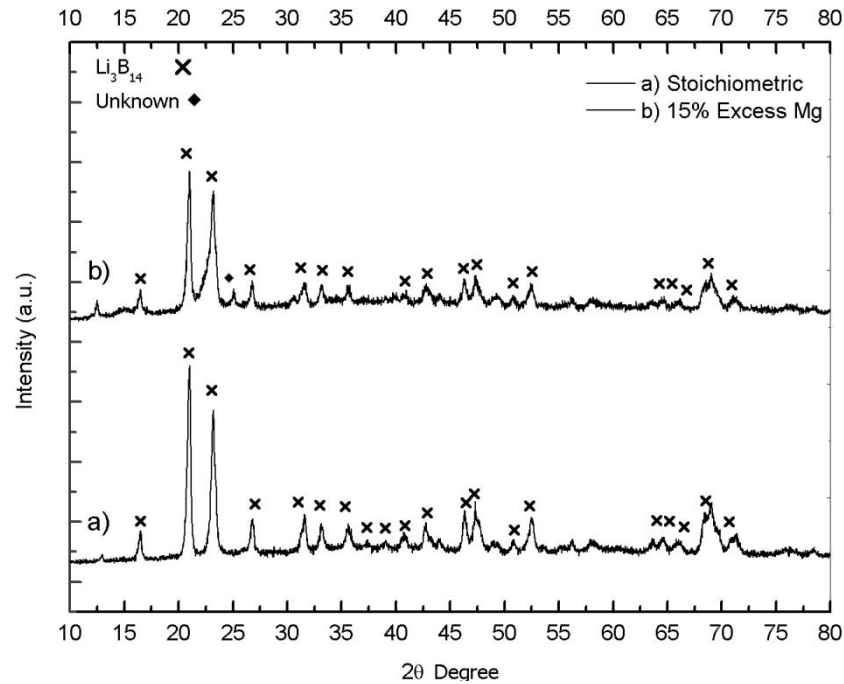


Figure 4.13. X-ray diagram of samples leached in 0.5 M HCl/water solution for 10 minutes a) Stoichiometric, b) 15% excess Mg addition

Figure 4.13 shows the leached products of samples in Figure 4.12. Samples were leached with 0.5M HCl/water solution for 10 minutes. It was observed that X-ray peak intensity values of the leached product with 15% excess magnesium were smaller than those measured for the peaks of stoichiometric sample. This was due to a decrease in the lithium boride amount in the product. Since BPR was constant for the experiments and mixture weights of the samples were the same, Li_2O and B_2O_3 amounts in

the mixture were lower in the 15% excess magnesium sample when compared to the stoichiometric sample. Also a new peak in the graph of sample Figure 4.13 (b) was observed. However, indexing of this peak could not be accomplished.

4.6 Variations in reactant mixture

In order to investigate the possibility of producing other lithium borides, different compositions for reactant mixture were tested. For this purpose, reactant mixture was prepared according to reaction (4.3). For comparison, it can be stated that this reactant mixture had 15% wt more Li₂O and 1.2% wt less B₂O₃ when compared to reaction (4.1). Comparison of the reaction mixtures is shown in Table 4.1.

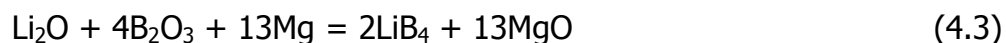


Table 4.1. Comparison of reaction mixtures (4.3) and (4.1)

Reaction	Li ₂ O, g	B ₂ O ₃ , g	Mg, g	Total
(4.3)	0.383	3.568	4.049	8.000
(4.1)	0.332	3.613	4.055	8.000

The mixtures were ball milled for 20 hours with 300 rpm and 30:1 BPR. Product of ball mill was leached in 0.5 M HCl/water solution for 10 minutes. XRD results are given for comparison with the product of reaction (4.1) in Figure 4.14. Graphs are labelled according to the reactant mixture.

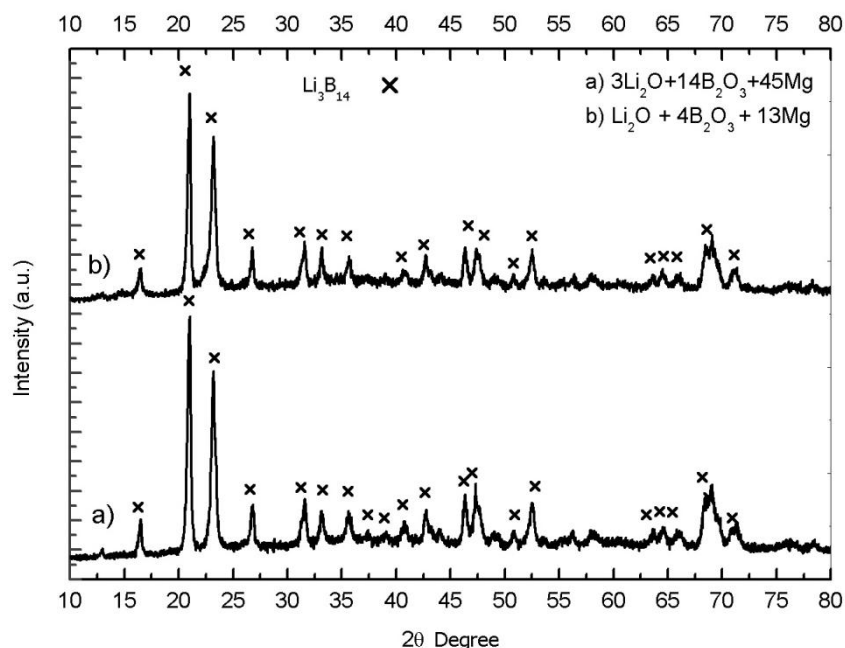


Figure 4.14. X-ray diagram of samples ball milled for 20 hours with 300 rpm and 30:1 BPR. Products were leached in 0.5 M HCl/water solution for 10 minutes a) Reaction (4.1), b) Reaction (4.3)

Figure 4.14 showed that there was not a new phase formation when the reactant mixture was prepared according to reaction (4.3). Therefore, X-Ray diffractogram of sample (b) was indexed as Li_3B_{14} . Also, a slight decrease in the peak intensity values of the sample (b) was observed.

In order to investigate the possibility of formation of other lithium borides by this method, the sample mixture was chosen such that reaction (4.3) would take place for different durations. Reactant mixtures were ball milled with 300 rpm and 30:1 BPR for 20, 30 and 60 hours. Results of milling prior to leaching are shown in Figure 4.15. Products of milling were leached in 0.5M HCl/water solution for 10 minutes. Results after leaching are shown in Figure 4.16.

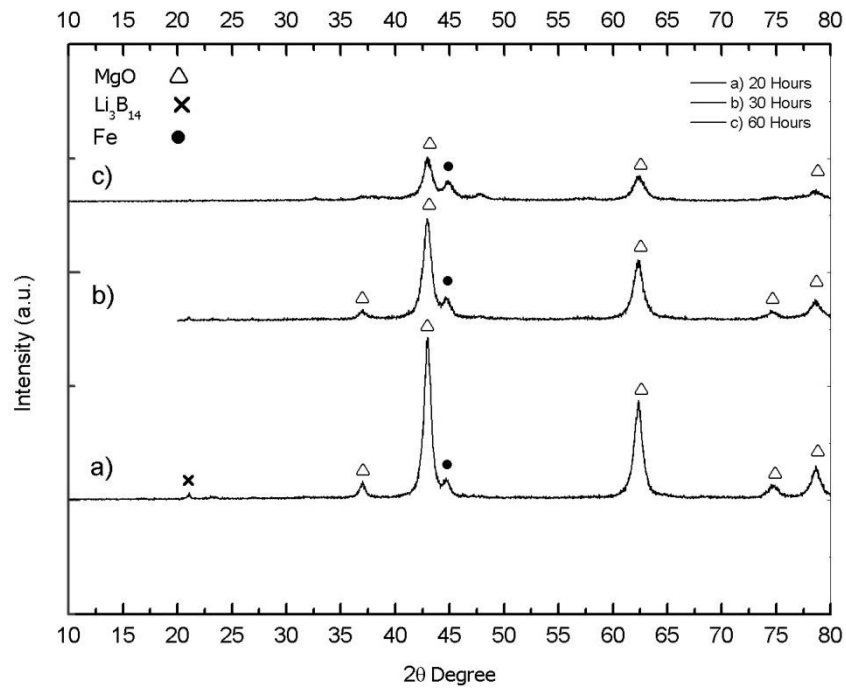


Figure 4.15. Samples were ball milled with 300 rpm and 30:1 BPR for a) 20 hours, b) 30 hours, c) 60 hours

As seen in Figure 4.15 crystal size of the samples decreased as the milling time increased which resulted in broadening and a decrease in height of the peaks. Iron contamination was observed in all samples. A characteristic peak of Li_3B_{14} was indexed in Figure 4.15 sample (a).

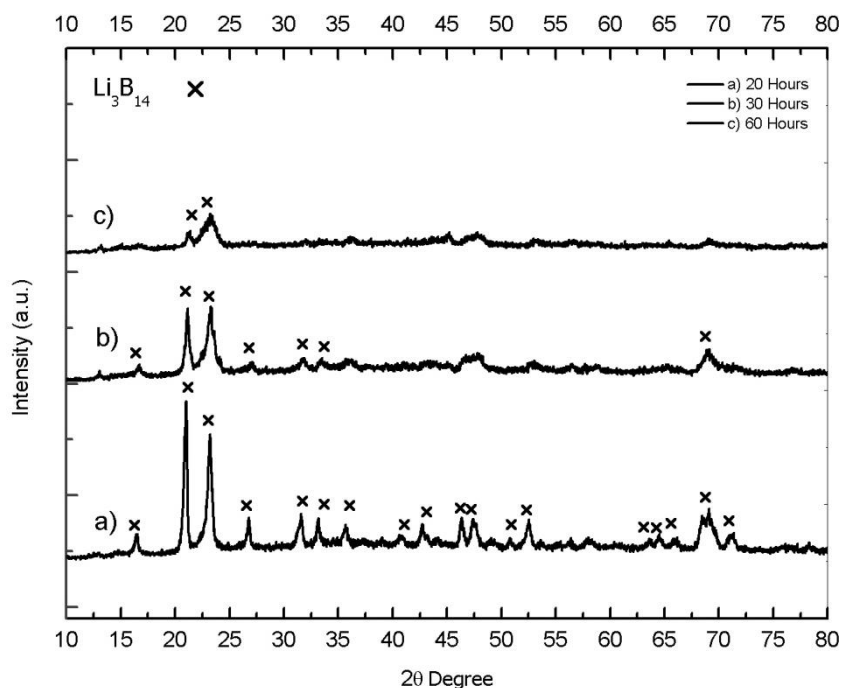


Figure 4.16. X-ray diagram for samples that were ball milled at 300 rpm and 30:1 BPR for a) 20 hours, b) 30 hours, c) 60 hours. Products of milling were leached with 0.5 M HCl/water solution for 10 minutes

An increase in the milling duration did not result in formation of a new compound as seen in Figure 4.16. As the milling time increased, crystal size of the sample decreased. Extreme ball milling durations could even cause a complete breakdown in crystal structure and formation of an amorphous structure⁽⁵⁹⁾.

Since increasing the energy input to the system did not show any new compound formation, experiments for shorter durations were done. Samples that were prepared according to reaction (4.3), were ball milled for 10 and 15 hours with 300 rpm and 30:1 BPR. X-ray diffraction analyses of products without leaching are shown in Figure 4.17.

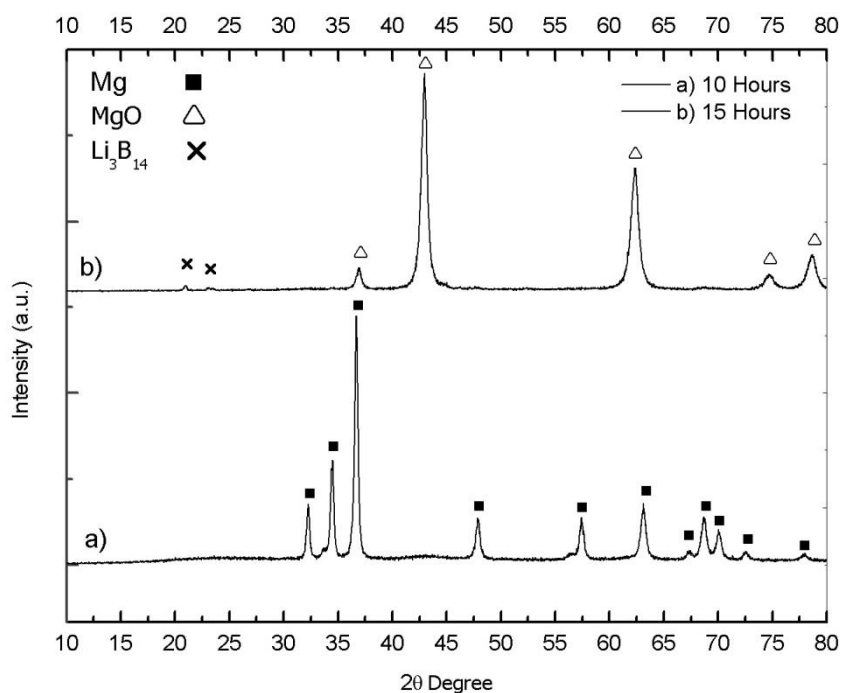


Figure 4.17. X-ray diagram of samples ball milled with 300 rpm and 30:1 BPR for a) 10 hours, b) 15 hours

No reaction took place at 10 hours of milling time and X-ray diffraction pattern of the sample showed only magnesium peaks. Figure 4.17 (b) shows the result of reduction reaction between Li_2O , B_2O_3 and Mg after 15 hours of ball milling. Two small peaks in the graph were indexed as Li_3B_{14} prior to leaching of the sample. Exact time of the reduction reaction could vary according to experimental parameters. However, 15-hour duration for this parameter was sufficient. In order to understand whether shorter milling duration resulted in a new compound formation or not, sample (b) was leached with 0.5 M HCl/water solution for 10 minutes and XRD pattern obtained was compared with that of a sample that was milled for 20 hours, as in Figure 4.18 (b).

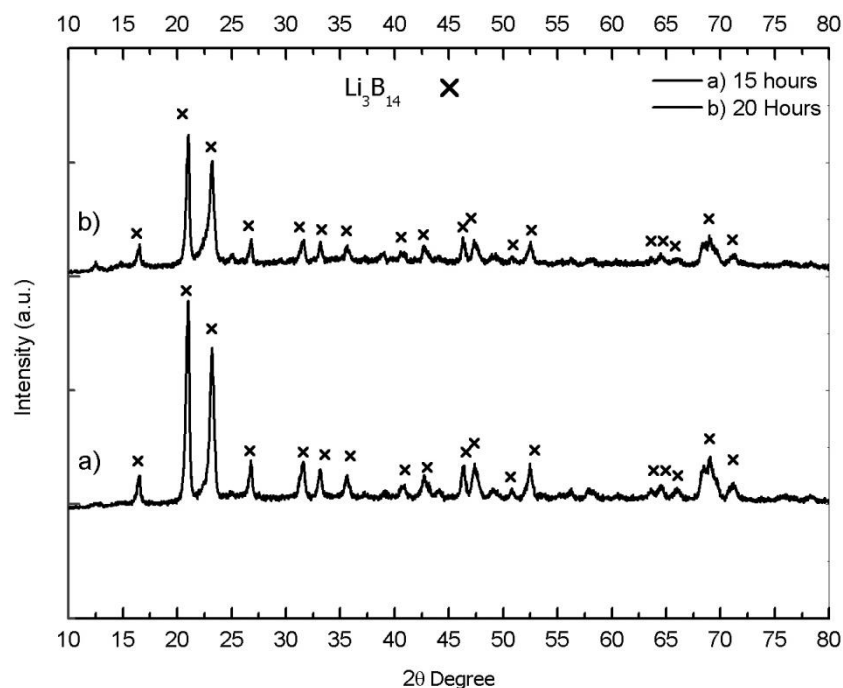


Figure 4.18. X-ray diagram of samples ball milled with 300 rpm and 30:1 BPR. Products of milling were leached with 0.5 M HCl/water solution for 10 minutes. Milling durations were a) 15 hours, b) 20 hours

Ball milling with low energy parameters did not result in a new compound formation as seen in Figure 4.18. XRD patterns of both samples are nearly identical.

Possible lithium boride formation with mechanochemical synthesis was also investigated for compounds that had more lithium when compared to Li_3B_{14} . Formation of Li_2B_6 was investigated according to reaction (4.4). However, Li_2B_9 peaks were observed in an experiment that was actually aimed to synthesise Li_2B_6 . Preparation of the reactant mixture was done according to reaction (4.4) with 30% excess Mg:



The reactant powder was ball milled for 20 hours at 300 rpm with 30:1 BPR. Ball milled powder was leached with 0.5 M HCl/water solution for 10 minutes. Indexing of peaks on the diffractogram was done according to the data reported by M. Panda in 2006. X-ray pattern of Li_2B_9 at 100°K that was reported by M. Panda is shown in Figure 4.19 ⁽⁴⁾.

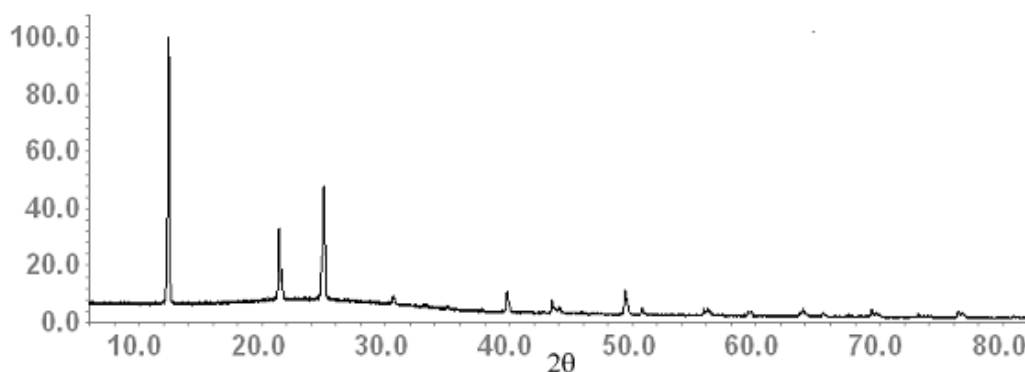


Figure 4.19. X-ray pattern of Li_2B_9 reported by M. Panda at 100°K ⁽⁴⁾

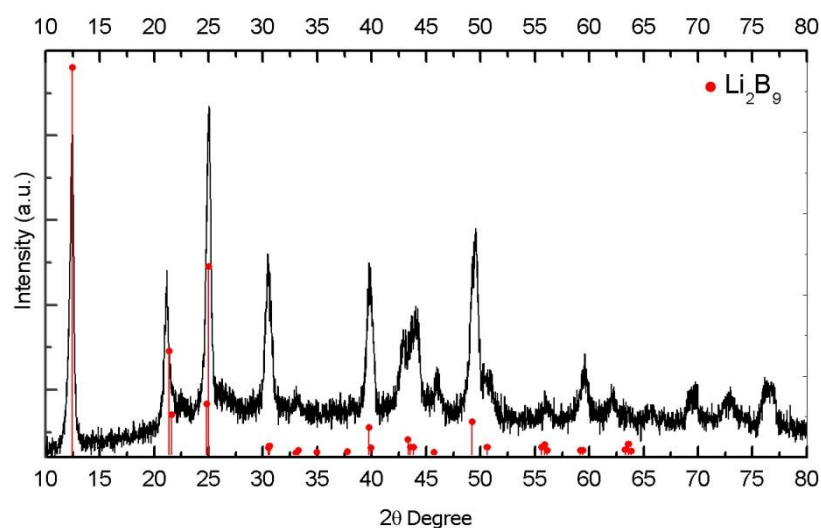


Figure 4.20. Comparison of Li_2B_9 literature data ⁽⁴⁾ with the observed data. Powder was ball milled for 20 hours at 300 rpm with 30:1 BPR and leached in 0.5 HCl/water solution for 10minutes

As seen in Figure 4.20, peaks observed were very similar to the peaks in data reported by Panda. Peaks above 65° were not indexed by Panda but when a comparison was made between the two diffractograms, similarity continued for unlabeled peaks as well. When the graphs were compared, high background intensity of the diffractogram in Figure 4.20 caused major intensity difference after 20°.

Possibility of synthesis a β -rhombohedral structured lithium boride with mechanochemical synthesis was also tested. Reactant mixture was prepared according to reaction (4.5):



The mixture was ball milled for 20 hours with 300 rpm and 30:1 BPR. Product of milling was compared with the stoichiometric Li_3B_{14} sample that was milled with the same parameters. Results of comparison are shown in Figure 4.21.

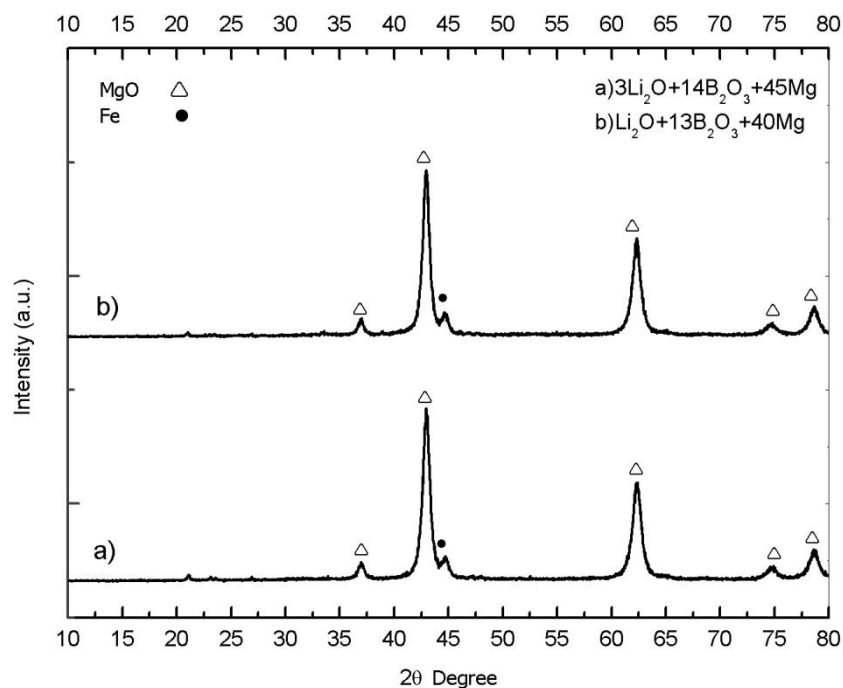


Figure 4.21. X-ray diagram for samples that were ball milled for 20 hours with 300 rpm and 30:1 BPR. a) Reaction (4.1), b) Reaction (4.5)

According to Figure 4.21, there was not a significant appearance of compositional difference. In fact, there was not a major change in the magnesium amount of reactant powders as given in Table 4.2. Therefore, X-ray diffraction patterns were almost identical. Products of milling were leached in 0.5 M HCl/water solution for 10 minutes. Leaching products of the above samples are compared in Figure 4.22.

Table 4.2. Comparison of reaction mixtures (4.5) and (4.1)

Reaction	Li ₂ O, g	B ₂ O ₃ , g	Mg, g	Total
(4.5)	0.125	3.797	4.078	8.000
(4.1)	0.332	3.613	4.055	8.000

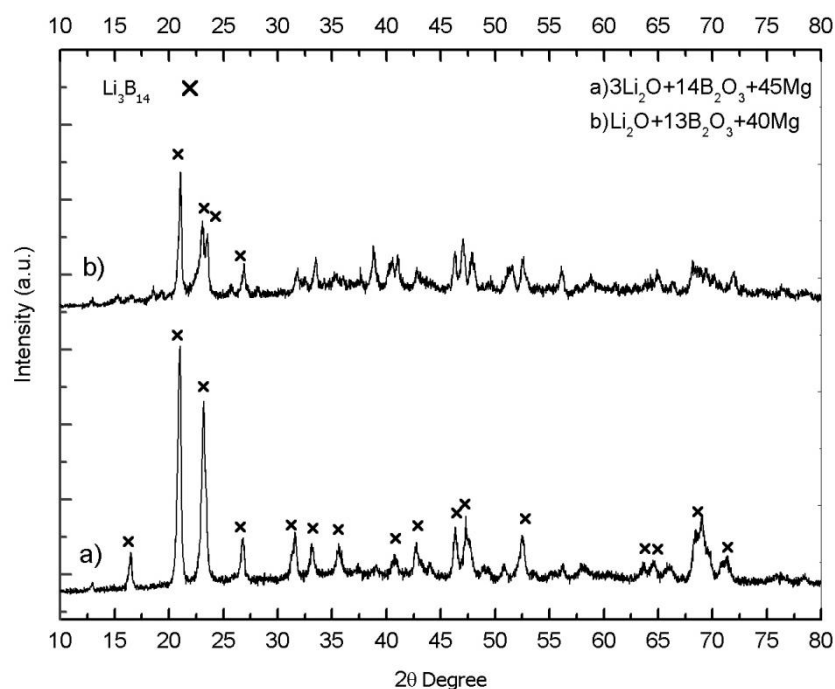
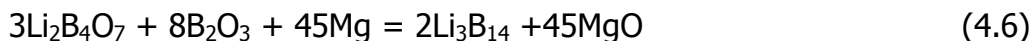


Figure 4.22. Samples were milled for 20 hours with 300 rpm and 30:1 BPR. Products were leached with 0.5 M HCl/water solution for 10 minutes. a) Reaction (4.1), b) Reaction (4.5).

After leaching of the samples, it was observed that β -rhombohedral structure did not form and also two peaks with the highest intensity fitted with the 2θ values of Li_3B_{14} structure. However, other peaks in the diffractogram could not be indexed due to the presence of another phase. Undefined peaks in sample (b) probably represent a different phase but it could not be characterized.

Synthesis route for Li_3B_{14} structure was also experimented by using a different reactant. $\text{Li}_2\text{B}_4\text{O}_7$ was used as lithium source in order to obtain a better understanding of mechanochemical synthesis of lithium borides. Reactant mixture was prepared according to reaction (4.6):



Reactant mixture that was prepared according to the above composition was subjected to ball milling for 20 hours with 300 rpm and 30:1 BPR. X-ray diffractogram of the sample was compared with the stoichiometric Li_3B_{14} synthesis with the same milling parameters. Comparison is shown in Figure 4.23.

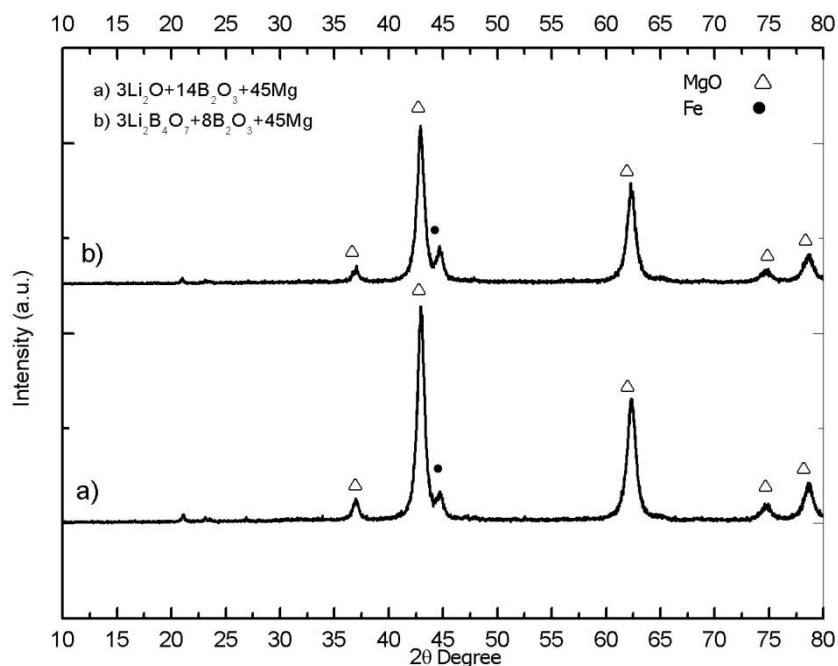


Figure 4.23. X-ray diagram of samples that were ball milled for 20 hours with 300 rpm and 30:1 BPR. a) Li_2O as lithium source, b) $\text{Li}_2\text{B}_4\text{O}_7$ as lithium source

MgO Intensity of sample (b) in Figure 4.23 was lower when compared with sample (a). However, both mixtures had the same amount of magnesium prior to milling. Intensity reduction of sample (b) can be explained by considering iron contamination of the samples. As seen in Figure 4.23 even though, MgO intensity values decreased, there was an increase in the iron

contamination of sample (b) when compared to sample (a). X-ray diffraction patterns showed that even if both samples were milled with the same parameters, for some reason sample (b) got more iron contamination. It was thought that an increase in the hardness of reactant mixture could cause such a change in the process products. B_2O_3 has a Mohs hardness of 4⁽⁷⁰⁾ and $Li_2B_4O_7$ has a Mohs hardness of 6-7⁽⁷¹⁾. Since $Li_2B_4O_7$ had a higher hardness when compared to B_2O_3 , milling with the same parameters probably increased the iron contamination of the product.

Effect of such compositional change was also investigated for the leached products. Above samples were leached in 0.5 M HCl/water solution for 10 minutes. Results are shown in Figure 4.24.

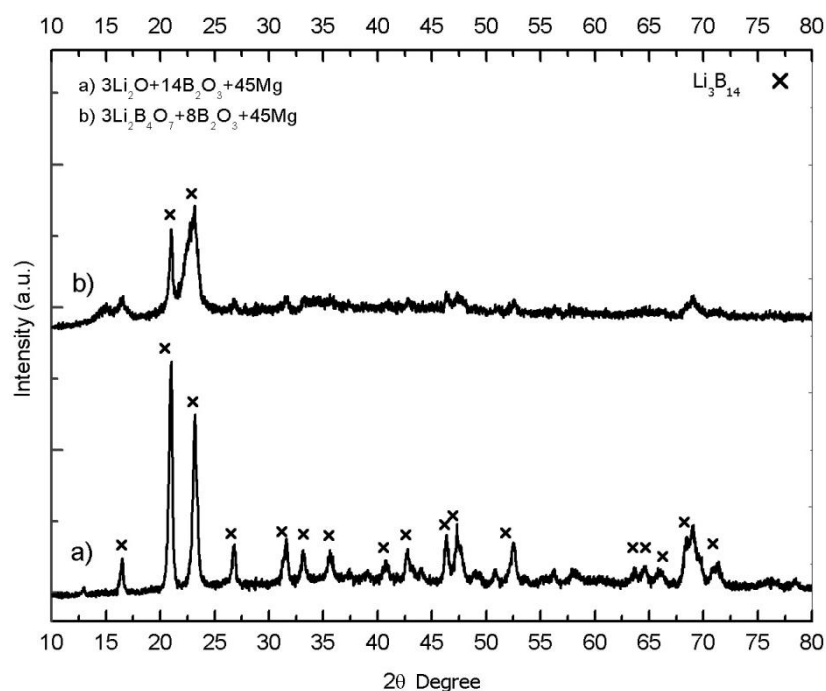


Figure 4.24. X-ray diagram of samples that were ball milled for 20 hours with 300 rpm and 30:1. Products of milling were leached in 0.5 M HCl solution for 10 minutes. a) Reaction (4.1), b) Reaction (4.6)

Only the highest intensity peaks of Li_3B_{14} were observed in Figure 4.24 for sample (b). Therefore, using a harder material as lithium source probably decreased the particle size more compared to reaction (4.1).

4.7 Other observations

Volume combustion synthesis for reaction (4.3) was tested to investigate the possibility of lithium boride formation. Experimental procedure explained in Akgün's study was used for volume combustion synthesis ⁽¹⁴⁾. Reactant mixture was ball milled for 20 minutes with 300 rpm to obtain proper mixing of reactants prior to the experiment. Then, it was poured into a graphite crucible and crucible was placed into the hot pot furnace that was described in Chapter 3. Experiment was performed under argon atmosphere. Reaction temperature was measured by a K-type thermocouple. X-ray analysis of the combustion reaction product is shown in Figure 4.25.

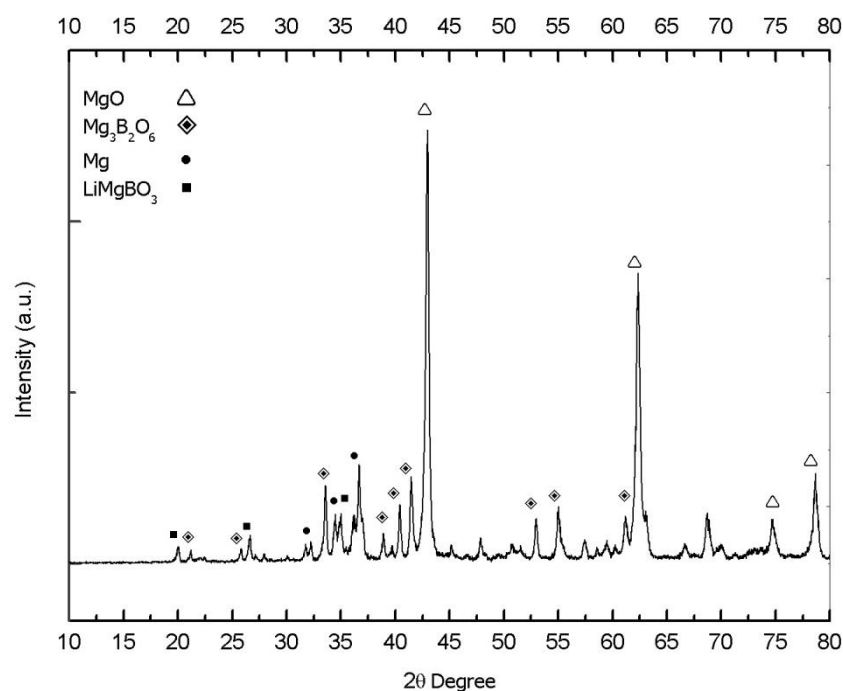


Figure 4.25. Indexing of volume combustion synthesis product

Volume combustion reaction took place at 810°C. XRD peaks of reaction products are shown in Figure 4.25. MgO, Mg₃B₂O₆, Mg and LiMgBO₃ peaks were observed after volume combustion reaction. Lithium boride formation was not observed in the product. In order to clean unwanted compounds from product powder, sample was leached in 1 M HCl solution for 15 hours. However, Li₃B₁₄ structure or other lithium boride formations were not observed after leaching. It was found that, leaching duration requirement for removal of Mg₃B₂O₆ was excessive. Even if, a Li₃B₁₄ formation had occurred in the powder, long leaching duration to remove Mg₃B₂O₆ caused lithium loss in Li₃B₁₄ structure ⁽⁸⁾. Long leaching durations is known to cause a collapse in Li₃B₁₄ structure and hinders the identification of the expected compounds ⁽⁸⁾.

CHAPTER 5

CONCLUSIONS

The aim of this study was to investigate the synthesis of lithium borides from oxides by mechanochemical production. Effects of ball milling parameters and leaching conditions were investigated. It was observed that reaction took place between 15th and 20th hours with 300 rpm and 30:1 BPR in synthesis experiments for Li_3B_{14} . Lower rpm values were experimented and reaction was not observed for 200 and 250 rpm. Increasing the energy input to the system by increasing rotational speed, BPR and milling duration resulted with a decrease in the product crystal size.

Fe and MgO were present in the reaction product with Li_3B_{14} . Different leaching durations and concentrations were experimented for elimination of these phases. It was found that leaching in 0.5 M HCl/water solution for 10 minutes was sufficient to remove Fe and MgO in the powder. Li_3B_{14} structure was observed in the leached products.

Process parameters that were found satisfactory to synthesize Li_3B_{14} were tested for other lithium boride compounds as well. LiB_4 , Li_2B_6 and LiB_{13} were tried to be synthesized. However, formation of these compounds was not observed after reactions. LiB_4 and LiB_{13} experiments resulted with XRD patterns similar to Li_3B_{14} . Also, Li_2B_9 peaks were observed in the reaction products of tests intended to synthesize Li_2B_6 .

Synthesis of Li_3B_{14} was tested with a different lithium source. $\text{Li}_2\text{B}_4\text{O}_7$ was added to the reactant mixture instead of Li_2O . Li_3B_{14} peaks were observed in XRD of product.

Volume combustion synthesis of Li_3B_{14} was also experimented. Reaction took place at 810°C . However, the formation of Li_3B_{14} or other borides was not observed in the products of both before and after leaching.

Future work suggestions:

- 1) Determination of critical ignition time can be done by using milling equipment with temperature measurement system.
- 2) In order to avoid iron contamination in the product, different ball mill equipment that is harder than reactants, can be used.
- 3) Products can be analyzed with suitable methods such as electron energy loss spectroscopy for both qualitative and quantitative analysis of light elements lithium and boron.

REFERENCES

1. It's Elemental. *Jefferson Lab*. <http://education.jlab.org/>, last visited on 7 January 2009
2. *The Economics of Boron*. London : Roskill Information Services Ltd., 2002.
3. *ETI Mine Works General Management*. General information about boron http://www.etimaden.gov.tr/tr/0_sayfa_ortakSayfa.asp?hangi_sayfa=4_sayfa_a_1 , last visited on 2 March 2009
4. P. Monalisa. *Ph.D.Thesis*. Hamburg : Universitat Hamburg, 2006.
5. *Web Elements Periodic Table*. <http://www.webelements.com/lithium/>, last visited on 7 January 2009
6. B. Post, Edit: R. M. Adams. *Boron, Metallo-Boron Compounds and Boranes*. New York : John Wiley & Sons, Inc., 1964.
7. A. Lipp, *Fr. Pat. Dec.* 9, 1, 461, 878, 1966.
8. G. Mair, R. Nesper, H. G. von Schnering. *J. Solid State Chem.* 75,30, 1988.
9. G. N. Srinivas, Z. Chen, T. P. Hamilton, K. Lammertsma. *Chemical Physics Letters*. 329, 239-247, 2000.
10. Ç. Çakanyıldırım, M. Gürü. *Renew. Energy*. doi:10.1016/j.renene.2008.01.015, 2008.

11. V. I. Matkovich, editor. *Boron and Refractory Borides*. New York : Springer-Verlag, 1977.
12. R. Thompson, Edit:R. J. Brotherton, H. Steinberg. *Progress in Boron Chemistry Volume 2*. Hungary : Pergamon Press, 1970.
13. R. Kiessling, *Acta Chem Scand*. 4,209-227, 1950.
14. A. Barış. *M.Sc. Thesis. METU*. 2008.
15. A. Meden, J. Mavri, M. Bele, S. Pejovnik. *J. Phys. Chem.* 99, 4252-4260, 1995.
16. H. Rosner, W. E. Pickett. *Phys. Rev. B* 67. 054104, 2003.
17. S. Orimo, Y. Nakamori, G. Kitahara, K. Miwa, N. Ohba, S. Towata et al. *J. Alloys Compds* . 404-406,427-30, 2005.
18. Y. Zhao, M. Zhang, S. Xu, C. Sun. *Chemical Physics Letters* . 432, 566–571, 2006.
19. J. J. Kaufman, L. M. Sachs. *J. Chem. Phys.* . 52, 645, 1970.
20. P. E. Cade, W. M. Huo. *At. Data Nucl. Data Tables*. 15, 1, 1975.
21. Z. H. Zhu, J. N. Murrell. *Chem. Phys. Lett.* 88, 262, 1982.
22. R. P. Saxon. *Theoretical Studies of Boron Compounds, Proceedings of the HEDM*. MA : Woods Hole, 1992.
23. J. A. Sheehy. *Spectroscopy of Lithium Boride, A candidate HEDM species. Proceedings of the HEDM*. MA : Woods Hole , 1995.
24. *8th Int. Pyrotechnics Seminar*. H. L. Lewis. CO USA : Steamboat Springs, 1982.

25. R. Naslain, J. Etourneau. *Comp. Rend.* 263 (6), 484, 1966.
26. R. Naslain, J. Etourneau, P. Hagemuller. *Bull. Soc. Chim. Fr.* 7, 2529, 1967.
27. P. Hagemuller, R. Naslain. *Compt. Rend.* 257,1924, 1963.
28. R.Naslain, J. S. Kasper, . *J. Solid State Chem.* 1,150, 1970.
29. R. Naslain, A. Guette, P. Hagemuller. *J. Less. Comm. Met.* 47,1, 1976.
30. B. Albert, *Angew. Chem. Int. Ed.* 37(8),1117, 1998.
31. B. Albert, K. Hofmann, Z. Anorg. *Allg. Chem.* 625,709, 1999.
32. B. Albert, *Eur. J. Inorg. Chem.* 2000(8), 1679, 2000.
33. B. Albert, K. Hofman, C. Fild, H. Eckert, M. Schleifer, R. Gruehn. *Chem. Eur. J.* 6(14),2531, 2000.
34. D. R. Secrist, *Ceram. Soc.* 50, 520, 1967.
35. Markowskii et al. *J. anorg. Chem. U.S.S.R.* 2, 34-41, 1957.
36. L. W. Rupp, Jr Debra J. Hodges. *J. Phys. Chem. Solids.* 35, 617-619, 1974.
37. S. D. James, L. E. DeVries. *J. Electrochem. Soc.* 123,321, 1976.
38. F. E. Wang, *U.S. Patent* 4,110,111. 1978.
39. F. E. Wang, M. A. Mitchell, R. A. Sutula, J. R. Holden, L. H. Bennett. *J. Less-Comm. Met.* 57, 161, 1978.
40. S. Dallek, D. W. Ernst, B. F. Larrick. *J. Electrochem. Soc.* 126, 866, 1979.

41. G. E. Mcmanis, A. N. Fletcher, M. H. Miles. *J. Electrochem Soc.* 134,286, 1984.
42. A. Meden, B. Pihlar, S. Pejonić. *J. Appl. Electrochem.* 24, 78, 1994.
43. S. Gunji, H. Kamimura. *Proc. 11th Int. Symp. Boron, Borides and Rel. Comp. JJAP Series.* 10,35, 1994.
44. S. Gunji, H. Kamimura. *The American Physical Society, Physical Review B.* 54,19, 1996.
45. B. Pevzner, Buckyball: a C₆₀ molecule. <http://www.godunov.com/Bucky/fullerene.html>. last visited on 6 December 2008
46. W. Hayami, T. Tanaka, S. Otani. *Journal of Solid State Chemistry.* 179, 2827–2833, 2006.
47. E. D. Jemmis, E. G. Jayasree. *Acc. Chem Res.* 36, 816-824, 2003.
48. M. Kobayashi, I. Higashi, H. Matsuda, K. Kimura. *J. Alloys Compd.* 221, 120-124, 1995.
49. R. C. Haddon, A. F. Hebard, M. J. Rosseinsky, D. W. Murphy, S. J. D'Amico, K. B. Lyons, B. Miller, J. M. Rosamalia, R. M. Fleming, A. R. Kortan, S. H. Glarum, A. V. Makhija, A. J. Muller, R. H. Eick, S. M. Zahurak, R. Tycko, G. Dabbagh, F. A. Thiel. *Nature.* 350,320, 1991.
50. I. I. Serebryakova, V. I. Lyashenko, V. D. Levandovskii. *Powder Metallurgy Met. Ceram.* 33,49, 1994.
51. H. G. von Schnering, G. Mair, M. Wörle, R. Nesper. *Z. Anorg. Allg. Chem.* 625,1207, 1999.
52. Z. Liu, X. Qu, B. Huang, Z. Li. *J. Alloys Compd.* 311, 256, 2000.

53. M. Wörle, R. Nesper, T. K. Chatterji. *Z. Anorg Allg Chem* . 632, 1737-1742, 2006.
54. H. B. Borgstedt, C. Gumirisk. *Journal of Phase Equilibria* . 24, 6, 2003.
55. Z. J. Liu, B.Y. Huang, Z. Y. Li. *Acta Metallurgica Sinica*. 17, 5, 667-671, 2004.
56. Z.J. Liu, B. Y. Huang, Z. Y. Li. *Acta Metallurgica Sinica*. 17, 5, 667-671, 2004.
57. L. Zi-jian, Y. Jian, M. Zhen-qiang, C. Jin, Z. De-bi. *Trans. Nonferroous Met. Soc. China*. 16(2006) 127-131, 2005.
58. K. Schmitt. *Ph.D. Thesis*. Justus-Liebig-Universität Giessen : s.n., 1997.
59. C. Suryanarayana, Mechanical alloying and milling. *Progress in Materials Science*. 2001, Vol. 46, 1–184.
60. G. B. Schaffer, P. G. McCormick. *Metall Trans*. A21, 2789-94, 1990.
61. L. Takacs. *Mater Lett*. 13, 119-24, 1992.
62. L. Takacs, L. *Mater Res Soc Symb Proc*. 286, 413-8, 1993.
63. G. B .Schaffer, P. G. McCormick. *Metall Trans*. A23, 1285-90, 1992.
64. P. G. McCormick, V. N. Wharton, M. M. Reyhani, G. B. Schaffer, Edit: D. C. Van Aken, G. S. Was, AK Ghosh. *Microcomposites and nanophase materials p. 65-79*. Warrendale : PA:TMS, 1992.
65. *"Materials and Material Analyses"*. Haan : Retsch GmbH, 2007.
66. *"Retsch Ball Mills Brochure"*. Haan : Retsch GmbH, 2007.

67. G. V. Arsdale, *Hydrometallurgy of Base Metals*. New York : The Maple Press, 1953.
68. F. Habashi *Principles of Extractive Metallurgy Volume 2 Hydrometallurgy*. New York, London, Paris : Gordon and Breach Science Publishers Ltd., 1970.
69. Lide, Editor: David R. *Hand book of Chemistry 73rd edition*. London : CRC Press, 1992-1993.
70. R. E. Kirk, J. I. Kroschwitz, D. F. Othmer, A. Seidel. *Kirk-Othmer Encyclopedia of Chemical Technology*. s.l. : J. Wiley, 2004.
71. S. J. Fan, 1993 IEEE International Frequency Control Symposium, 1993. 353-358.